Dynamics of bacterial communities in a pilot scale methane biofilter

by

Misha D. Miazga-Rodriguez

A thesis submitted in partial fulfillment of the requirements for the degree of

Master of Science

in

Microbiology and Biotechnology

Department of Biological Sciences
University of Alberta

Abstract

Methane is the second most important greenhouse gas after carbon dioxide with a global warming potential over 100 years 25 times that of CO_2. Today, anthropogenic sources of methane comprise 60% of the global methane budget per year and tools for mitigating emissions have become increasingly important to limit climate change. One such tool is methane biofilters (MBF) which utilize biological metabolism, mainly the metabolism of methane oxidizing bacteria (MOB), to scrub methane. To date, the majority of research on MBFs has focussed on the physical aspects of biofilter function rather than the biological component. In this study, bacterial and MOB communities in a pilot scale MBF were studied over the course of a year to assess how these communities change over time and in response to the presence or absence of CH_4. The bacterial and MOB communities were assessed by analyzing 16S rRNA and methane monooxygenase subunit A (*pmoA*) genes using DGGE, T-RFLP, RFLP, and qPCR methodologies. The MBF bacterial community composition changed in response to the presence or absence of methane. The MOB community composition was unaffected by methane input; the dominant community members being related to the *Methylomicrobium* and *Methylobacter* genera and lower abundance members belonging to the *Methylocaldum* and *Methylocystis* genera. The size of the bacterial community and the MOB community was numerically larger when methane was present and smaller when methane was absent. Enrichment experiments yielded a MOB related to the *Methylomicrobium* genus. No published studies could be found that presented both *pmoA* sequence data or provided general bacterial community information from a functional pilot scale MBF as a function of methane input. Hence, the data from this

study add new information to our understanding of bacterial community dynamics in a pilot scale MBF.

Acknowledgements

I must first thank my supervisor Dr. Lisa Stein for taking me into her lab at the last minute and supporting my work for the past three years. Dr. Stein's guidance, advice, and patience has, without a doubt, made me a better scientist.

Next I thank my supervisory committee, Dr. Julia Foght and Dr. Ian Buchanan for their valuable advice. Thank you to Dr. Buchanan for giving me the opportunity to work with his lab on the biogas-methane biofilter project and thanks to his PhD student Vahid Razaviarani for providing the gas flow data shown in this report. Thank you Dr. Foght's lab members Nidal Abu Laban, Carmen Li, and Boonfei Tan for their expert help with protocols and data analysis.

I would like to give my thanks to my past and present lab mates. Special thanks to Jessica Kozlowski, Mohammad Ghashghavi, and Catharine Tays for their advice and support. A big, huge thanks to Reem Skeik, Dimitri Kits, and Albert Remus-Rosana for helping me with my experiments. Thanks to Dimitri for helping me with MOB enrichments and always offering great advice. Thanks to Albert for helping me with T-RFLP and qPCR experiments and showing me what good science is all about.

I extend a big thanks to Dr. Brian Lanoil and his past and present lab members for all their advice, help, and guidance.

I have to give a special thank you to my father who not only supported me mentally in this little endeavour, but also helped me out with sampling gas and soil from the MBF and by giving me rides from the University to Goldbar and back.

Lastly, I have to thank my Mom, my brother Chris, my wonderful girlfriend Sarah, and all my friends. Thank you to everyone for supporting me and believing in me.

Table of Contents

List of Figures.....ix

List of Tables.....x

List of abbreviations.....xi

1.0 INTRODUCTION 1

1.1 Methane and Planet Earth.....1

1.1.1 A brief history of methane on Earth.....1

1.1.2 Sources, sinks and reservoirs of methane.....3

1.1.3 Methane clathrates and the tipping point of Climate Change.....5

1.1.4 Mitigating methane emissions.....6

1.2 The Diversity of the Methanotrophs.....6

1.2.1 The four phyla of methane oxidizing bacteria.....8

1.2.2 The diversity of MOB in methane biofilters.....11

1.3 The Physiology of Methanotrophs.....12

1.3.1 MOB Methane Monooxygenases.....13

1.3.2 The MOB Methane Oxidation Pathway.....17

1.3.3 The assimilation of carbon from the methane oxidation pathway....18

1.3.4 MOB Assimilation of Carbon via the CBB Cycle.....22

1.3.5 Fermentation of Methane, via formaldehyde, by MOB.....22

1.3.6 Nitrogen Assimilation by MOB 25

1.4 Methane Biofilters: Function and Form 26

1.4.1 Methane Supply into Biofilters.....26

1.4.2 Assessment of Biofilter Matrix Composition.....28

1.4.3 Aeration of Methane Biofilters.....29

1.4.4 Temperature and Moisture Effects on Methane Biofilters.....31

1.4.5 Nitrogen Effects on Methane Biofilters.....33

1.4.6 Volatile Sulfur Compound Effects on Methane Biofilters.....34

1.4.7 Phosphate and Metal Requirements in Methane Biofilters.....35
1.5 The Goldbar Biofilter.....36
1.6 Objective and Hypotheses.....39
2.0 METHODS.....38
2.1 Soil and Gas Sampling.....39
2.1.1 Soil Sampling from the Methane Bofilter.....39
2.1.2 Gas Sample from the Methane Biofilter.....40
2.2 Nucleic Acid Extractions and Purifications.....43
2.2.1 DNA extraction from biofilter compost: Griffith Extraction.....43
2.2.2 Additional sephadex G200 purification of extracted DNA.....44
2.2.3 Ethanol precipitation of DNA.....45
2.2.4 Gel purification of *pmoA* amplicon using Qiaquick Gel Extraction Kit 46
2.2.5 Purification of amplicon using Qiagen column purification kit.....47
2.2.6 Genomic DNA extraction from cultivated cells.....47
2.3 Polymerase Chain Reaction Protocols.....48
2.3.1 Amplification of the bacterial 16S rRNA gene for DGGE.....49
2.3.2 Amplification of the bacterial 16S rRNA gene for RFLP.....50
2.3.3 Amplification of the bacterial 16S rRNA gene for TRFLP.....50
2.3.4 Amplification of the *pmoA* gene for RFLP.....50
2.3.5 Amplification of the *pmoA* gene for TRFLP.....51
2.3.6 Amplification of the insert from Pcr2.1 plasmid by colony PCR.....52
2.3.7 Sanger diDeoxy sequencing using BigDye reaction mix.....52
2.3.8 Quantitative PCR.....52
2.4 DNA Electrophoresis.....55
2.4.1 Agarose gel electrophoresis.....55
2.4.2 Denaturing gradient gel electrophoresis.....55
2.5 Restriction Fragment Length Polymorphism.....57

2.5.1 Cloning of PCR Amplicon into PCR 2.1 Topo Vector.....57

2.5.2 Transformation of PCR 2.1 TOPO Vector into chemically competent Top10 *E. coli*.....57

2.5.3 Blue-white screening of transformants and recombinants.....58

2.5.4 Enzymatic Digest of PCR amplified insert.....58

2.5.5 RFLP Pattern Analysis and Sequencing.....59

2.6 Terminal Restriction Fragment Length Polymorphism.....59

2.6.1 Klenow Fragment Treatment.....59

2.6.2 Enzymatic digest of amplicon to generate T-RFs.....60

2.6.3 DNA 3730 T-RF sequencing.....60

2.7 Gas Chromatography.....62

2.8 DNA Quantification.....62

2.9 Bioinformatic Analysis.....63

2.9.1 Sequence analysis by BLAST.....63

2.9.2 Phylogenetic analysis of *pmoA* and 16S rRNA gene sequences.....63

2.9.3 DGGE analysis by Gel Compar II.....63

2.9.4 Statistical Analysis of Metagenomic Profiles (STAMP) of T-RFLP..64

2.10 Enrichment of MOB from Goldbar methane biofilter.....64

3.0 RESULTS.....67

3.1 Measurements of methane, carbon dioxide and gas flow at the methane biofilter.....67

3.2 Temporal study of the methane biofilter bacterial assemblage.....71

3.2.1 Biological observations of the methane biofilter.....71

3.2.2 DGGE analysis of the bacterial assemblage.....71

3.2.3 TRFLP analysis of the bacterial assemblage.....72

3.3 Methane oxidizing bacterial assemblage in the methane biofilter.....77

3.3.1 Phylogenetic analysis of *pmoA* clone library sequences.....77

3.3.2 Temporal dynamics of the MOB assemblage in the methane biofilter 78

3.4 Enrichment of MOB native to the methane biofilter.....81

3.5 Quantification of the total bacterial and MOB community in the methane biofilter.....83

4. DISCUSSION.....85

4.1 The effect of methane input on the methane biofilter bacterial assemblage.....85

4.2 The effect of methane input on the MOB assemblage.....92

4.3 Future Experiments.....95

4.4 Conclusions.....96

5. References.....98

List of figures

1.0 INTRODUCTION

Figure 1.1 MMO phylogenetic tree showing the evolutionary relationships of pMMO, AMO, and pXMA.....10

Figure 1.2 The central aerobic methane oxidation pathway.....16

Figure 1.3 The Ribulose Monophosphate carbon assimilation.....20

Figure 1.4 The serine carbon assimilation pathway.....21

Figure 1.5 Pathway of the EMP-variant of the RuMP pathway in *M. alcaliphilum* str. 20Z.....24

Figure 1.6 Diagram of upflowing biofilter accompanied by chemocline data.....27

Figure 1.7 Schematic of the pilot scale biogas generators and methane biofilter at Goldbar.....38

2.0 METHODS

Fig 2.1 The methane biofilter located at the Goldbar Waste Water Treatment Plant.....41

3.0 RESULTS

Figure 3.1 Measurements of methane and carbon dioxide input into the methane biofilter.....69

Figure 3.2 Gas flow measurements of gas produced from anaerobic digesters.70

Figure 3.3 DGGE fingerprinting of the bacterial assemblage over time.....74

Figure 3.4 PCA analysis of the bacterial assemblage by T-RFLP fingerprinting of 16S rDNA.....75

Figure 3.5 Heatmap analysis of the bacterial assemblage by T-RFLP fingerprinting of 16S rDNA.....76

Figure 3.6 Phylogenetic analysis of *pmoA* clones from the methane biofilter and MOB enrichment.....79

Figure 3.7 Phylogenetic analysis of the 16S rDNA MOB clone the methane biofilter MOB enrichment.....82

Figure 3.8 Quantification of *pmoA* and 16S rDNA from the methane biofilter by qPCR.....84

4.0 Discussion

Figure 4.1 The City of Edmonton monthly temperature and precipitation.....91

List of Tables

1.0 INTRODUCTION

Table 1.1 Current extant phyla and genera of methanotrophic organisms from the domain *Bacteria* and *Archaea*.....9

2.0 METHODS

Table 2.1 Soil samples collected during the lifespan of the methane biofilter.....42

Table 2.2 Table of primers.....54

Table 2.3 Table of restriction endonucleases.....61

Table 2.4 Composition of the MOB enrichment media, nitrate mineral salts.....66

3.0 RESULTS

Table 3.1 Temporal variation of the MOB assemblage by RFLP.....80

4.0 DISCUSSION

Table 4.1 Shannon-Wiener diversity index analysis of bacterial communities....89

Table 4.2 Estimation of the average percent MOB in the total bacterial community in the MBF.....90

List of Abbreviations

µl	microlitre
ADP	adenosine diphosphate
AMO	ammonia monooxygenase
ANOVA	analysis of variance
ATP	adenosine triphosphate
BLAST	basic local alignment search tool
BSA	bovine serum albumin
CTAB	cetyl trimethylammonium bromide
CytC	cytochrome C
DGGE	denaturing gradient gel electrophoresis
DNA	deoxyribonucleic acid
dNTP	deoxy nucleotide triphosphate
EDTA	ethylenediaminetetraacetic acid
EMP	Embden–Meyerhof–Parnas (pathway)
EPS	exopolysaccharide
FalDH	formaldehyde dehydrogenase
FAM	5-fluorescein
FDH	formate dehydrogenase
FU	fluoresence units
GB	Goldbar
GC	gas chromatography
GC-TCD	gas chromatography - thermal conductivity detector
IAA	isoamyl alcohol
L/hr	litres per hour
LB	lysogeny broth
max.	maximum
MBF	methane biofilter
MBSU	molecular biology services unit
MDH	methanol dehydrogenase
MEGA	Molecular Evolutionary Genetics Analysis
mg	milligrams
ml	millilitres

mM	millimolar
MOB	methane oxidizing bacteria
mRNA	messenger ribonucleic acid
N	nitrogen
NADH	nicotinamide adenine dinucleotide
NEB	New England Biolabs
NMS	nitrate mineral salts
OD	optical density
OTU	operational taxonomic unit
PCA	principal comparison analysis
PCR	polymerase chain reaction
PEG	poly ethylene glycol
PETM	paleocene-eocene thermal maximum
Pfk	phosphofructokinase
PGA	glyceraldehyde-3-phosphate
PHB	poly-3-hydroxybutyrate
pMMO	particulate methane monooxygenase
PPi	pyrophosphate
PQQ	pyrroquinoline quinine
qPCR	quantitative polymerase chain reaction
RFLP	restriction fragment length polymorphism
RFU	relative fluorescence units
RNA	ribonucleic acid
rRNA	ribosomal ribonucleic acid
RT	room temperature
RuMP	ribulose monophosphate pathway
SDS	sodium dodecyl suphate
sMMO	soluble methane monooxygenase
SOC	super optimal broth with catabolite repression
STAMP	Statistical Analysis of Metagenomic Profiles
TAE	tris-acetate EDTA
TE	tris EDTA
TEMED	tetramethylethylenediamine
TET	5-tetrachloro-fluorescein
T-RF	terminal-restriction fragment
T-RFLP	terminal-restriction fragment length ploymorphism
UPGMA	unweighted pair group method with arithmetic mean

V	volts
v/v	volume per volume
v/w	volume per weight
VSC	volatile sulphur compound

1. INTRODUCTION

1.1 Methane and Planet Earth

Methane gas is a pillar of modern human society. The diverse use of methane by humans spans from fuel sources for automobiles and planes, to home heating and power generation, to a key role as a reactant in the Haber-Bosch process, the chemical synthesis of nitrogen mineral fertilizers. Despite methane's many uses, it is a potent greenhouse gas 25 times more effective than carbon dioxide and excessive methane emission could further alter Earth's climate (1). Therefore it is important to humanity that methods of minimizing anthropogenic methane emission be developed and implemented to mitigate climate change and the potential dangerous consequences of climate change.

This introduction will summarize the history of methane research, the influence of methane on Earth's global climate, the diversity and physiology of methane oxidizing bacteria (MOB), technologies for mitigating methane release into the atmosphere from human activities, and finally how my thesis research integrates into other research efforts.

1.1.1 A brief history of methane on Earth

The discovery of methane is attributed to Alessandro Volta in 1778 and independently a few years later by John Dalton. Both Volta and Dalton had discovered biologically generated methane and ultimately characterized this new gas based on its flammable properties and the "whooshing" sound the gas produced when combusted (2) . Dalton later theorized the first (and ultimately incorrect) molecular structure of

methane and named it “carburretted hydrogen” giving methane the molecular structure of CH_2 (2). Today we now know the molecular structure of methane to be CH_4 and apart from the myriad of modern day uses, methane is the most abundant organic molecule in the atmosphere and a major contributor to ozone degradation and global warming. While methane is less abundant than carbon dioxide in the atmosphere, it absorbs heat more effectively than carbon dioxide and is estimated to be 25 to 30 times more potent than carbon dioxide as a greenhouse gas in its global warming potential over 100 years (1, 2).

Pre-industrially, the factors affecting methane concentrations in Earth’s atmosphere were originally thought to be purely influenced by natural processes, however current research has demonstrated that humanity’s influence on atmospheric methane likely extends into our pre-historical past. But, how do researchers measure atmospheric methane going back hundreds if not hundreds of thousands of years? The story of Earth’s gassy past is stored in thousand year old ice at Earth’s North and South poles. When the ice froze in the ice caps it locked within it the atmospheric gas at the time of freezing; essentially sampling the atmosphere. To retrieve this sample locked in ice, ice cores are drilled and sections of the core are analysed for the gases present within it. The deeper the depth the ice core is drilled to, the further back in time researchers can peer (3).

This methodology has revealed some surprising results, mainly that the concentration of methane in Earth’s atmosphere was likely influenced by humans as long as 5000 years ago (4). Since no large scale industry existed at this time, researchers pondered how it was possible for pre-industrial man to influence the

composition of Earth's atmosphere (4, 5). The most probable answer rests with one of humanity's most important staple foods, rice. Rice paddies used for rice farming are essentially human made, or anthropogenic, wetlands and are an ideal environment for the main biological generator of methane gas, methanogens from the domain Archaea (4–7). Today, rice paddies contribute 10% of the methane to Earth's yearly global methane budget while wetlands contribute 23%, the single largest source of methane on Earth (8).

Since the industrial revolution atmospheric methane concentrations have skyrocketed from approximately 725 parts per billion (ppB) (around 1700 AD) to nearly 2000 ppB in the present day. We now know that the combined anthropogenic contribution to the global methane budget exceeds all natural sources, comprising more than 60% of the global methane budget of about 500-600 Tg of methane per year (1, 4, 8).

1.1.2 Sources, Sinks and Reservoirs of Methane

Despite this massive increase in atmospheric methane since the advent of the industrial revolution, the majority of methane, around 70%, is still derived from microbial sources via methanogenesis (8). Methanogenesis is the reduction of carbon dioxide to methane by anaerobic methanogenic archaea and is a final and very important step in the degradation of organic molecules. The methanogenesis biochemical pathway utilises the products of fermentation: hydrogen gas, carbon dioxide, some small organic acids (such as acetate or formate), methylamines, and methylsuphides creating methane as a waste product of their metabolism (9–11). Two example biochemical

pathways for methanogenesis are carbon dioxide and formate reduction. The pathways are complex, but they can be simplified to two chemical equations:

$$CO_2 + 4H_2 \rightarrow CH_4 + 2H_2O \quad \Delta G^{o'} = -131 \text{ KJ/mol (9, 10)}$$

$$4HCOO^- + 4H^+ \rightarrow CH_4 + 3CO_2 + 2H_2O \quad \Delta G^{o'} = -120 \text{ KJ/mol (10)}$$

Methanogenesis occurs in anaerobic zones in aquatic, marine, and soil environments. An increasingly large proportion of methane in the global methane budget is being derived from abiogenic sources, such as fossil fuel use and biomass burning (18% and 7% of total methane budget, respectively) (8). Agricultural processes, mainly rice and livestock farming, are still the single largest contributor of methane, nearly 27% of the global methane budget (8).

A major reservoir of methane is in structures called methane hydrates, also known as clathrates. Clathrates are found in the ocean floor subsurface and are composed of water ice and methane gas encapsulated in bubbles within the ice. Estimates of the amount of methane contained within the clathrates vary, but current literature estimates that anywhere between 500,000 and 10,000,000 Tg of methane is held within the icy cage of the clathrates (8). This is between 10,000 and 20,000 times the amount of the current global methane budget (8). Methanotrophs, organisms that consume methane as a carbon and energy source, remove much of the methane as it is slowly released from the clathrates. Methanotrophs are the single largest sink of methane on Earth and are immensely important at mitigating atmospheric levels of methane (8).

1.1.3 Methane clathrates and the Tipping Point of Climate Change

Methane released from clathrates is a possible positive feedback mechanism of global warming, the mechanism being that as ocean temperatures rise the clathrates melt and release large amounts of methane. This large methane release over a short period of time will overwhelm methanotrophs that consume methane from clathrates, allowing the methane to escape into the atmosphere. This large methane release will further warm the oceans through greenhouse gas effects, stimulating additional methane release from clathrates and other sources resulting in the positive feedback loop (12–14). This has been dubbed the tipping point model and evidence in Earth's distant past indicates that the mass release of methane from clathrates may be responsible for large increases in Earth's global temperature (12–14).

These major increases in temperature have happened throughout Earth's history and are characterized by rapid warming over very short geological time scales. One of the first major increases in temperature that was likely as a result of clathrate destabilization occurred about 635 million years ago (15). This temperature increase occurred at the probable termination of "snowball Earth," a point in geological history where the planet was theorized to be almost completely covered with ice (15). Another rapid warming event that has been attributed, at least in part, to clathrate destabilization was approximately 183 million years ago during the early Jurassic period and was accompanied by mass extinction of both ocean and land flora and fauna (16). The most recent rapid warming event, the Palaeocene-Eocene thermal maximum (PETM), occurred approximately 55 million years ago, where global temperatures rose more than 6^{o}C (17). Like the early Jurassic warming event, the PETM was accompanied by the

mass extinction of ocean and land flora and fauna (17). Computer modeling of current rates of global warming indicate that the possibility of a tipping point scenario, where the destabilization and mass release of methane occurs, is a real threat and may be occurring presently (14, 18). To avoid rapid climate change in the future, actions must be taken presently to reduce humanity's contribution to greenhouse gases such as carbon dioxide, methane, and nitrous oxide.

1.1.4 Mitigating Methane Emissions

To reduce the anthropogenic contribution of methane, information of the systems to target and the technologies for emissions reductions must be compiled. Some potential targets of methane reduction include landfills, waste water treatment plants, and animal husbandry operations. These operations worldwide combine to contribute nearly 30% of the total yearly methane budget (8). These operations have become the target of research into methane mitigation technologies. Typically, three mechanisms are used to minimize the release of methane gas from these operations: flaring (the burning of methane), collection of methane for use as a biogas, and the use of methane biofilters (MBF), the focus of this review. Methane biofilters rely on the activity of methanotrophs and are increasingly being employed to treat polluted gas before release into the environment. To understand how the biofilters function and how they may be optimized, it is important to understand the methanotrophs.

1.2 The Diversity of the Methanotrophs

The first organism known to science that was capable of growth from the oxidation of methane was discovered by N.L. Sohngen in 1906 from pond water and

aquatic plants; he dubbed his new isolate *Bacillus methanicus* (2). Unfortunately, *B. methanicus* was lost to science and no new isolates were discovered until 1966 when J.W. Foster and Richard H. Davis were able to re-isolate *B. methanicus* (renaming it *Pseudomonas methanica*) and isolate a new species, *Methylococcus capsulatus* (2, 19). These organisms were dubbed methane-utilizing bacteria and subsequent work by luminaries in the field of microbiology, such as Roger Whittenbury, resulted in the isolation of dozens of new species of methane-utilizing bacteria, which would later on be known as “methane oxidizing bacteria” (MOB) or simply as “methanotrophs” (2).

Today, researchers continue to isolate methanotrophs from a wide range of environments at different extremes of numerous physico-chemical parameters including extremes in pH and temperature. This has revealed an even greater genetic diversity of methanotrophs than previously thought, necessitating a classification system to organize methanotrophs. The species of methanotrophs discovered by Sohngen and Foster and Davis were subsequently classified as belonging to the domain *Bacteria*. The original classification of aerobic methanotrophs was into three groups titled: type I, type II and type x (20). This classification scheme is based on numerous physiological characteristics that will be discussed later on in this introduction (20).

In recent years there has been a shift to classifying methanotrophs based purely on the phylogeny of the 16S ribosomal RNA (rRNA) gene sequence. This shift in classification scheme is a reflection of the increasing diversity of methanotrophs since their original discovery and a movement in the field of microbiology away from classifying bacteria and archaea purely on physiological features. Despite this shift, many authors still utilize the now outmoded classification scheme when describing

methanotrophs and examples can be found in literature as recently as 2013 (21, 22). A useful molecular marker for the detection of MOB in the environment is the *pmoA* gene. The *pmoA* gene is a subunit of the enzyme particulate methane monooxygenase (pMMO), a key enzyme in the methane oxidation pathway and is found in all species of MOB except for the genus *Methylocella* (for more information see section 1.3.1).

1.2.1 The Four Phyla of Methane Oxidizing Bacteria

Methanotrophs are now known to be represented in four phyla in the domain *Bacteria* and one phylum in the domain *Archaea* (see Table 1 and Figure 1) based on the analysis of 16S rRNA genes. The reclassification of methanotrophs based on rRNA genes also allows researchers to establish evolutionary relationships between different methanotroph species. What were once considered to be type I and type X methanotrophs are now purely classified based on the class that all type I and type x methanotrophs reside, *Gammaproteobacteria* within the phylum *Proteobacteria*. Similarly, type II MOB are part of the class *Alphaproteobacteria* and phylum *Proteobacteria*.

Recently novel methanotrophs from the domain *Bacteria* have been isolated from the phylum *Verrucomicrobia* in 2007-2008 (23–25) and the phylum NC10 in 2009 (26). These new methanotrophs are not only phylogenetically distinct, but also physiologically distinct with unique pathways for carbon fixation and methane oxidation which will be discussed briefly in the physiology section of this review. These new methanotrophs speak to the widening diversity of organisms utilizing methane as an energy and/or carbon source and the ubiquity of methanotrophic microbes on Earth.

Table 1.1 Extant phyla and genera of methanotrophic organisms from the domain *Bacteria* and *Archaea* in pure culture

	Domain	Phylum	Current Extant Genus Names			
Aerobic Methanotrophs	Bacteria	*Gammaproteobacteria* (Formerly Type I)	*Methylomonas* *Methylobacter* *Methylomicrobium*	*Methylosoma* *Methylovulum* *Methylosarcina*	*Methylohalobius* *Methylothermus* *Methylococcus*	*Crenothrix** *Methylocaldum*
		Alphaproteobacteria (Formerly Type II)	*Methylosinus*	*Methylocystis*	*Methylocapsa*	*Methylocella*
		Verrucomicrobia	*Methylacidiphilum* **			
Anaerobic Methanotrophs	Bacteria	NC-10	*Methylomirabilis****			
	Archaea	Euryarchaeota	No species in pure culture			

Adapted from Bowman 2011 (113). *(114),**(23–25), ***(115)

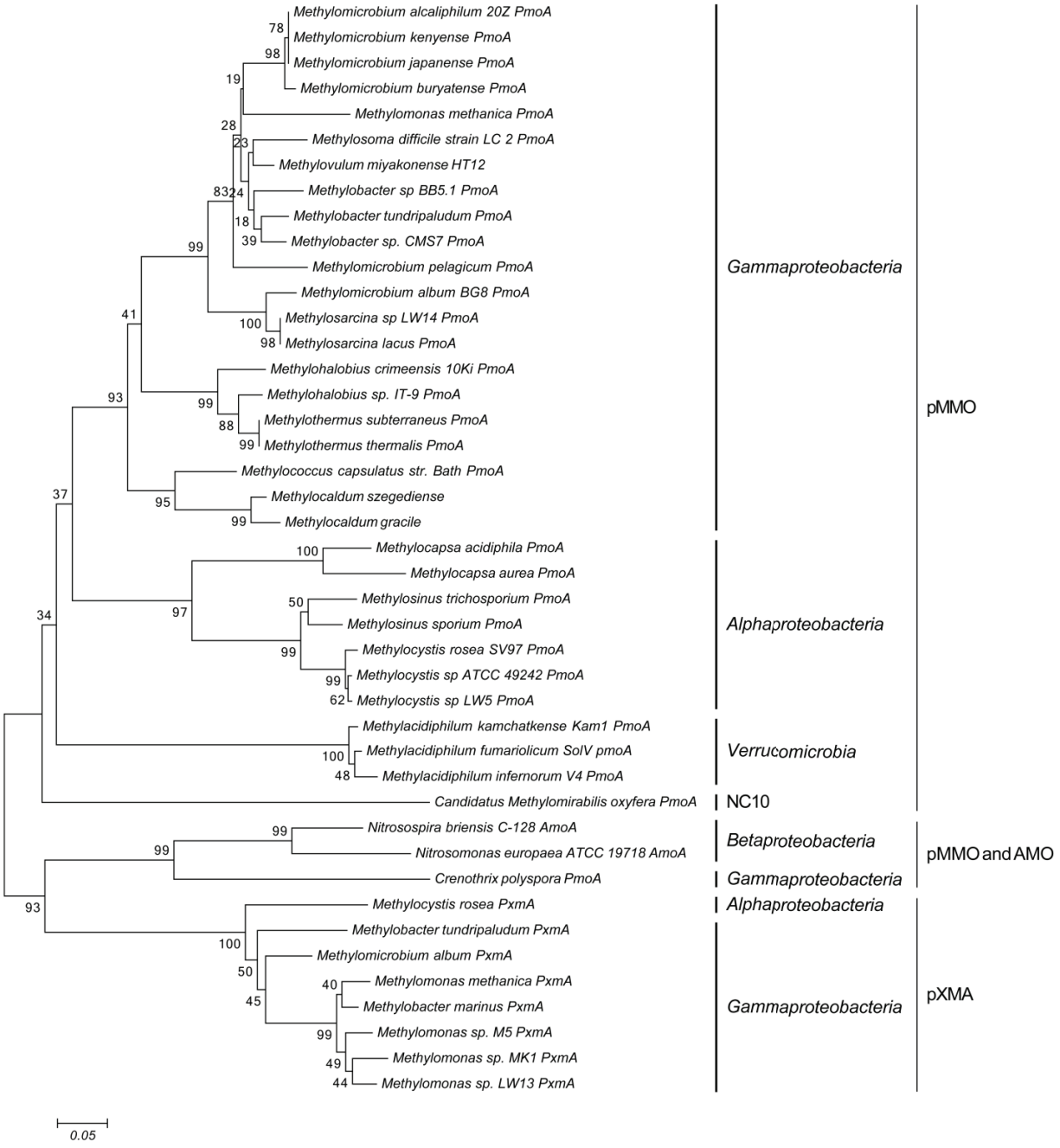

Fig 1.1 MMO phylogenetic tree showing the evolutionary relationships of pMMO, AMO, and pXMA monooxygenase amino-acid neighbour-joining tree constructed using MEGA 5.2. **pMMO** (particulate methane monooxygenase), **AMO** (ammonia monooxygenase), and **pXMA** (pMMO-like monooxygenase) are shown (see section 1.3.1). The percentage of replicate trees in which the associated taxa clustered together in the bootstrap test (10,000 replicates) are shown next to the branches. A total of 149 amino acid residues was analyzed for this tree.

1.2.2 The Diversity of MOB in Methane Biofilters

In methane landfill cover soil, proteobacterial methane-oxidizers (MOB) are the only methanotrophs that have been detected. In mature cover soils *Alphaproteobacteria* MOB, in particular members of the genus *Methylocystis*, tend to dominate the methanotroph soil assemblage over *Gammaproteobacteria* as surveyed by Gebert *et al.* in two studies of MOB in landfill cover soil (27, 28). An additional analysis by Gebert *et al.* confirmed their previous observations of the dominance of *Alphaproteobacteria* MOB in cover soil (29).

While *Alphaproteobacteria* MOB tend to dominate older cover soils, Jugnia *et al.* discovered that *Gammaproteobacteria* dominated recently implemented cover soils (30). Jugnia *et al.* hypothesized that this discrepancy between their study and the previous studies by Gebert *et al.* indicate that *Gammaproteobacteria* may be the pioneering MOB of cover soils, dominating until *Alphaproteobacteria* MOB are able to establish themselves in the cover soil (30). While this is an attractive theory, it is problematic to generalize the response of a group of physiologically and genetically diverse MOB classes. Further long term research on the maturation of cover soils should be conducted to confirm if there is a trend of pioneering by *Gammaproteobacteria* MOB followed by the establishment of *Alphaproteobacteria* MOB.

Only one attempt has been made to isolate methanotrophs from biofilter soils and characterize the isolates (31, 32). In two studies, Wise *et al.* first isolated two novel methanotrophs from a landfill cover soil methane biofilter and then characterized their physiology (31, 32). The two novel species of methanotrophs were classified in the

genus *Methylosarcina* (32). No studies since have described novel species of methanotrophs from methane biofilters and so the physiological nature of MOB from biofilters remains largely unstudied.

Though MOB from the phyla *Verrucomicrobia* or NC10 have never been detected in methane biofilters, the possibility of the existence of MOB from these phyla cannot be ruled out. This is especially true because the primers used in previous molecular studies of methane biofilters would not have been able to detect the highly divergent *pmoA* (Fig. 1.1). New primers capable of detecting *Verrucomicrobia* or NC10 MOB have recently been designed and as more isolates of each phyla are discovered, the primers can be improved to detect a broader range of methanotrophs from these phyla (33, 34). Future studies assessing the diversity of MOB communities in any environment should include *Verrucomicrobia* or NC10 primers if a thorough assessment of diversity is to be made.

1.3 The Physiology of Methanotrophs

As discussed in the introduction, methanotrophs extract carbon and energy from methane. Though the overall reaction can simplified to:

$$CH_4 + 2O_2 \rightarrow CO_2 + 2H_2O + e^- \qquad \Delta G^{o'} = -780 \text{ kJ/mol}$$

it is important to understand each step in the process. Knowledge of the underlying processes allows researchers to anticipate and explain behaviour seen in individual methane oxidizing bacteria and in MOB assemblages.

1.3.1 MOB methane monooxygenases.

The initial step of methane oxidation is catalyzed by the enzyme methane monooxygenase (MMO) (see Figure 1.2 for complete pathway). There are two types of MMO currently known in MOB. They are known as soluble methane monooxygenase (sMMO) and particulate methane monooxygenase (pMMO) and were initially differentiated based on centrifugation. When centrifuged, sMMO remains in solution while pMMO is pelleted. The properties of the MMOs are due to the localization of each MMO type in the MOB cell. pMMO is membrane bound, associated with intracellular membranes found in MOB. sMMO, on the other hand is associated with the cytoplasm. Until recently, sMMO was better characterized than pMMO due to the relative ease by which the protein was able to be crystallized for x-ray crystallography. In the last decade scientists have finally been able to analyze the crystal structure of pMMO from the species *Methylocystis* sp. strain M, *M. capsulatis* Bath, and *M. trichosporium* OB3b (35–38).

pMMO can be found in all MOB in both *Alpha*- and *Gammaproteobacteria* except for members of the genus *Methylocella,* which only contain sMMO (39). sMMO can be found in genera in both *Alpha*- and *Gammaproteobacteria*, but it is not universal. pMMO and sMMO are evolutionarily distinct and have different mechanisms for the oxidation of methane. pMMO requires copper ions as cofactors while sMMO utilizes iron cofactors. The determining factor for the expression of sMMO or pMMO in an MOB that can express either is the availability of copper. When copper is limited in the environment, sMMO will be expressed. When copper is not limiting, the “copper-switch” is activated and pMMO will be expressed while the expression of sMMO will be repressed (40–42).

Like their evolutionary origin, pMMO and sMMO have distinct substrate ranges. sMMO is known to have a broader range and is capable of oxidizing a variety of hydrogenated carbon compounds such as: alkanes, alkenes, and aromatics (43, 44). pMMO is relatively more specific for methane than sMMO and as such MOB expressing pMMO tend to outcompete those expressing sMMO. This is due to competition for the active site of sMMO between methane and other hydrocarbons. This limits the ability for sMMO expressing MOB to convert methane into energy for growth. In addition, growth is also limited by the accumulation of toxic products produced as a result of the degradation of some hydrocarbon compounds, such as halogenated hydrocarbons (45).

Due to the central role copper plays as a cofactor for pMMO and as a regulator of sMMO/pMMO expression the demand for copper in MOB is high when compared to other organisms. Copper demand has been calculated to be 10-fold greater than other microorganisms and as such MOB require mechanisms to concentrate copper from its surrounding environment into its cytoplasm (40, 41). The gathering of copper from the environment occurs through the action of siderophore like proteins known as chalkophores. MOB secrete these chalkophores, known as methanobactin, into the surrounding environment which increases the bioavailability of copper (40, 41).

Recent work has uncovered another potential MMO. This putative MMO has been dubbed pXMO and is related, but distinct from other known monooxygenases (Fig. 1.1). The physiological function of pXMO has not yet been ascertained, but the *pxmA* gene encoding a subunit of the protein is present in some genera in both *Alphaproteobacteria* and *Gammaproteobacteria* MOB (46, 47) . The *pxmA* subunit A gene has been detected by PCR and by metagenomic sequencing in two environments:

sphagnum mosses and oilsands tailings ponds (46–48). In addition, mRNA transcripts from the pXMO *pxmABC* operon have been detected in both sphagnum mosses and in pure culture MOB, suggesting that the monooxygenase is utilized and is not simply an evolutionary relic (46, 47).

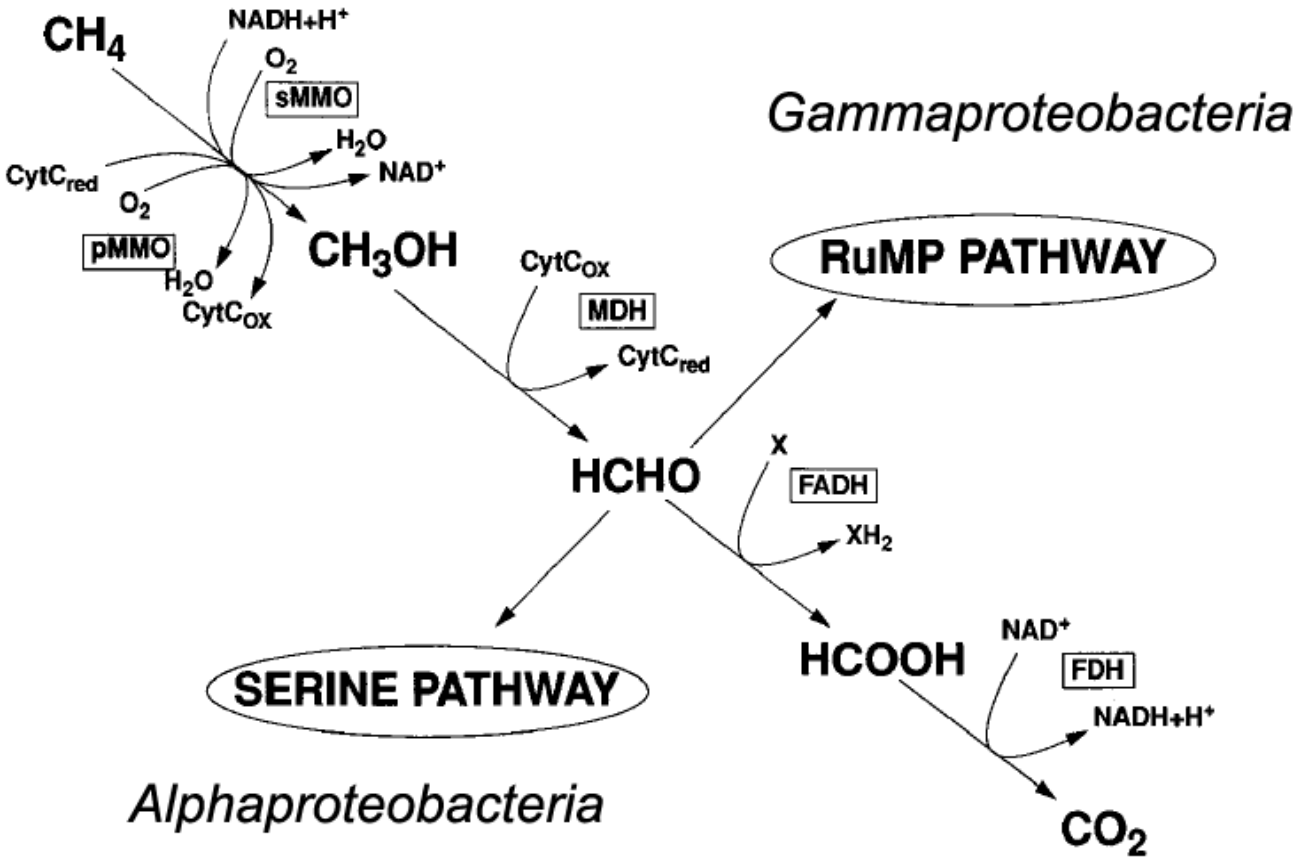

Figure 1.2 The central aerobic methane oxidation pathway from Hanson and Hanson, 1996 with alterations. **pMMO** (particulate methane monooxygenase), **sMMO** (soluble methane monoxygenase), **MDH** (methanol dehydrogenase), **FalDH** (formaldehyde dehydrogenase), **FDH** (formate dehydrogenase), **CytC** (cytochrome C.).

1.3.2 The MOB Methane Oxidation Pathway

The initial step in the methane oxidation pathway is an energy investment step requiring two electron equivalents and molecular oxygen to oxidize methane to methanol (CH_3OH) (Fgure 1.2). For pMMO, the energy input for oxidation comes from a cytochrome *c* (*cytC*). For sMMO, the energy input is received from NADH + H^+. Methanol is subsequently oxidized to formaldehyde (HCHO) by the enzyme methanol dehydrogenase (MDH). The oxidation of methanol generates one electron of energy. The canonical MDH utilized by MOB is designated as the MxaF-type and until recently was the only MDH thought to be used by MOB.

Recent work has shown that another MDH recently characterized in the methylotroph *Methylobacterium extorquens* AM1 and found in many species such as *Rhodobacter sphaeroids, Paracoccus denitrificans*, *Methylotenera mobilis* JLW8 and *Methylobacterium radiotolerans* is present in the verrucomicrobial methanotroph, *M. fumariolicum* SolV (49–54). This MDH, known as XoxF-type, has been demonstrated to have the extremely unusual property of using lanthanum and other lanthanides as metal cofactors instead of calcium, which is used in MxaF-type MDH (54, 55).

Once the carbon has been oxidized to formaldehyde the pathway branches into two possible routes (figure 1.2). The carbon can either continue to be oxidized and generate energy via the dissimilatory methane oxidation pathway or be incorporated into cell biomass via one of two possible assimilatory pathways. In the dissimilatory pathway, formaldehyde is oxidized to formate ($HCOO^-$) by the enzyme formaldehyde dehydrogenase (FalDH) generating another electron. FalDH is an enzyme with diverse forms. In general, FalDH can be categorized into two broad groups: the $NAD(P)^+$ -

dependent FalDH and dye-linked FalDH (56). $NAD(P)^+$ - dependent FalDH is cytoplasmic and is often linked to other factors such as thiol compounds, tetrahydrofolate, methylene tetrahydromethanopterin, and a variety of modifier proteins affecting the activity and specificity of the enzyme. Dye-linked FalDH, named for its detection by dye reduction, is linked to cytochromes, such as pyrroquinoline quinine (PQQ) and is membrane bound. Both types can be found in *Alpha*- and *Gammaproteobacteria* and sometimes both types can be found within one species (20, 56, 57). FalDH expression is also known to be regulated by copper (41).

Finally, formate is oxidized to carbon dioxide in the final energy-generating step by the enzyme formate dehydrogenase (FDH).

1.3.3 The assimilation of carbon from the methane oxidation pathway

There are two possible assimilatory pathways available for the incorporation of carbon, from formaldehyde, into cell biomass. The ribulose monophosphate (RuMP) pathway is utilized by *Gammaproteobacteria* MOB (Figure 1.3). The serine pathway is utilized by *Alphaproteobacteria* MOB (Figure 1.4).

The RuMP receives its name from the initial step in the pathway where formaldehyde is combined with ribulose monophosphate to form hexulose-6-phosphate (Fig. 1.3). An interesting implication of the RuMP pathway is the mechanism of carbon storage or dumping. *Gammaproteobacteria* divert carbon into exopolysaccharide (EPS) synthesis in the event of excess carbon and low nutrients, primarily nitrogen (58). The synthesis pathway is not well understood, but it appears that only *Gammaproteobacteria* are capable of dumping excess carbon into EPS to prevent the

accumulation of formaldehyde intracellularly (58). Understanding the mechanisms of EPS synthesis is important for biofilters due to possibility of clogging apparatuses with excess EPS.

The serine pathway receives its name from the first reaction of the pathway where formaldehyde reacts with glycine to produce serine (20). *Alphaproteobacteria* do not seem to be able produce a large amount of EPS, but research into this is limited (58). It is known that carbon from the serine pathway can be diverted into polyhydroxybutyrate (PHB) synthesis. PHB is stored intracellularly and provides a mechanism by which *Alphaproteobacteria* MOB can recover from starvation more rapidly than MOB that do not store PHB. Despite earlier work showing otherwise, all known *Gammaproteobacteria* MOB are incapable of producing PHB (59, 60). The ability of *Alphaproteobacteria* to produce PHB may be directly related to the serine pathway (60). Carbon for PHB synthesis is diverted from the serine cycle at the acetyl-CoA step (59).

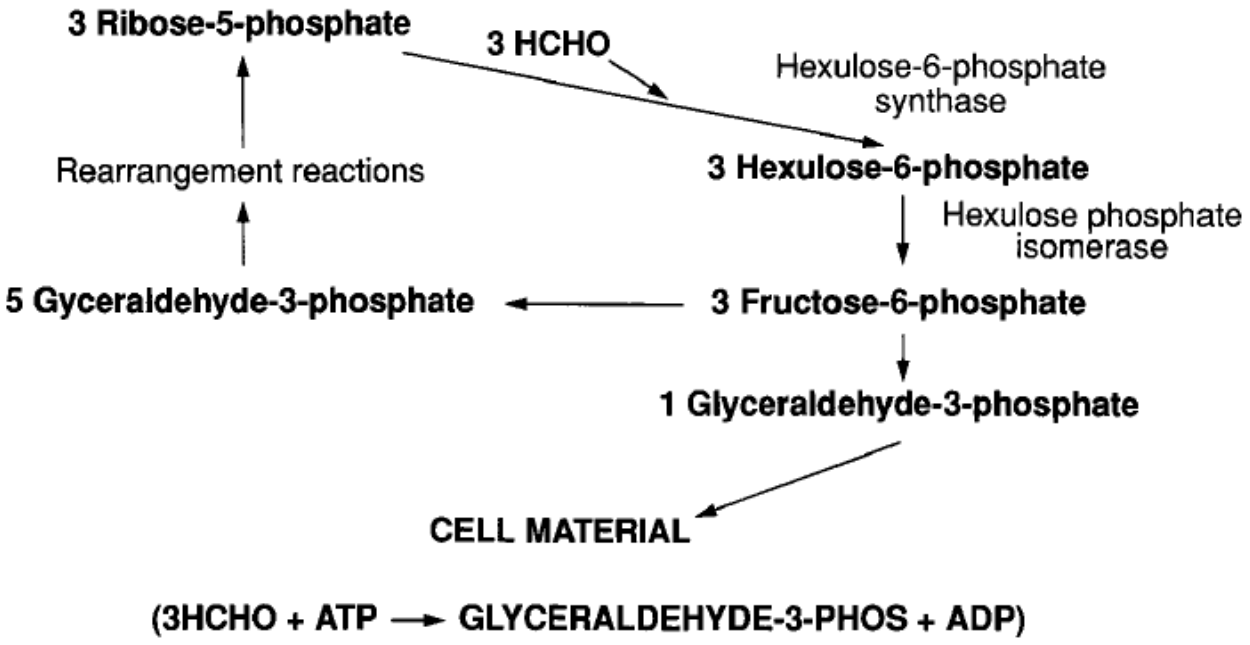

Figure 1.3 The Ribulose Monophosphate carbon assimilation pathway from Hanson and Hanson, 1996 **Phos** (Phosphate)

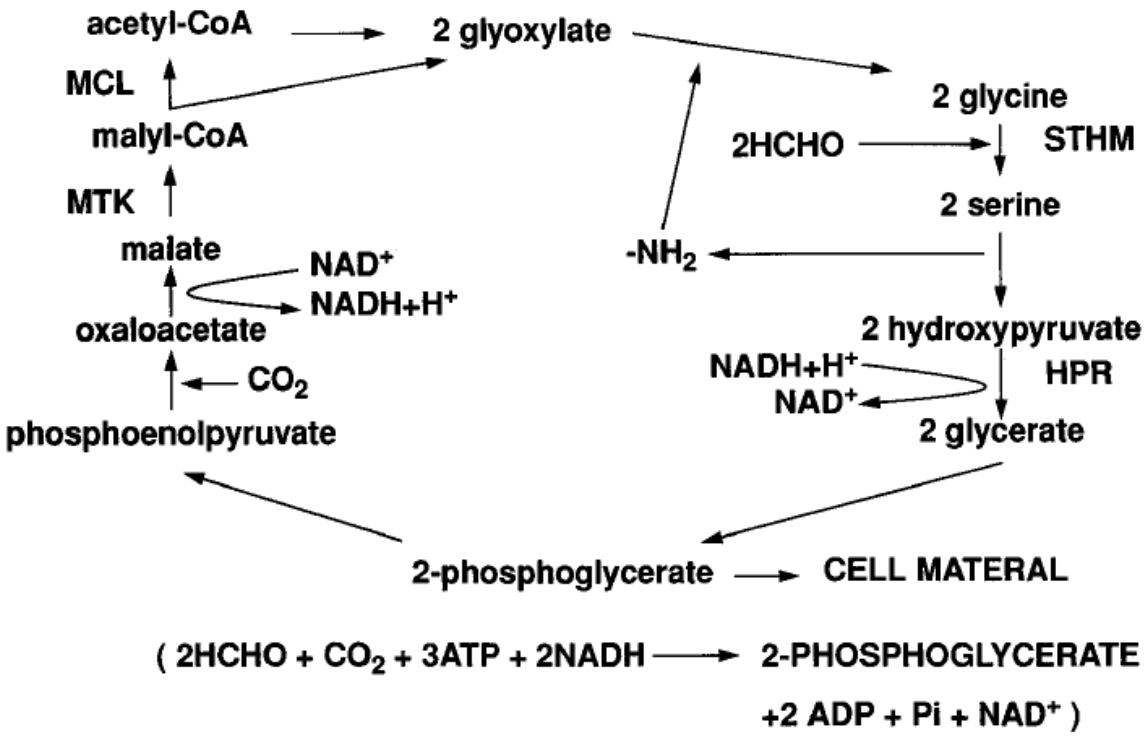

Figure 1.4 The serine carbon assimilation pathway from Hanson and Hanson, 1996. Serine hydroxymethyl transferase (STHM), Hydroxypyruvate reductase (HPR), Malate thiokinase (MTK), malyl coenzyme A lyase (MCL)

1.3.4 MOB Assimilation of Carbon via the CBB Cycle

The serine pathway and RuMP pathway are not the only mechanisms by which methanotrophs can assimilate carbon into their biomass. Genes for carbon assimilation via carbon dioxide are also present in some *Gammaproteobacteria*. *Methylococcus capsulatus* Bath encodes in its genome the genes for the Calvin Benson Bassham Cycle (CBB) (61). It appears that *M. capsulatus* Bath is capable of growing without methane by fixing carbon dioxide into its biomass and using hydrogen gas (H_2) or formate as a reduced energy source (61). To this date, very few studies have been published on autotrophy in proteobacterial methanotrophs.

Recently, methanotrophs from the phylum *Verrucomicrobia* and the candidate phylum NC10 were discovered to not encode genes for either the serine or RuMP pathway (25, 62). Instead, these methanotrophs are obligate autotrophs, deriving their carbon from the CBB cycle and their energy from the oxidation of methane via the classical methane oxidation pathway (25, 62, 63). Additionally, *Verrucomicrobia* methanotrophs store carbon intracellularly as glycogen (64). Lastly, species of *Alphaproteobacteria* in the genera *Methylocella, Methylocapsa,* and *Methylocystis* are known to be facultative methanotrophs (65). These organisms are capable of growing on organic carbon (such as acetate, ethanol, and malate) or methane (65). They have so far only been found in acidic environments, such as acidic peat bogs (65).

1.3.5 Fermentation of Methane, via formaldehyde, by MOB

Recent work has demonstrated a novel metabolism used by the MOB *Methylomicrobium alcaliphilum* str. 20Z. *M. alcaliphilum* is capable of fermenting

methane, via formaldehyde, by the glycolytic (EMP) pathway (Figure 1.5). Previous to this study there were several apparent lesions in the EMP pathway of *Gammaproteobacteria* methanotrophs, among them the lack of a phosphofructokinase and a pyruvate kinase. The discovery of divergent forms of pyruvate kinase and pyrophosphate-dependent phosphofructokinase resolved these lesions. The EMP pathway was found to be active under hypoxic conditions and growth via the pathway was observed indicating that *M. alcaliphilum* is able to assimilate carbon and gain energy via this fermentative pathway from methane instead of hexose sugars (66).

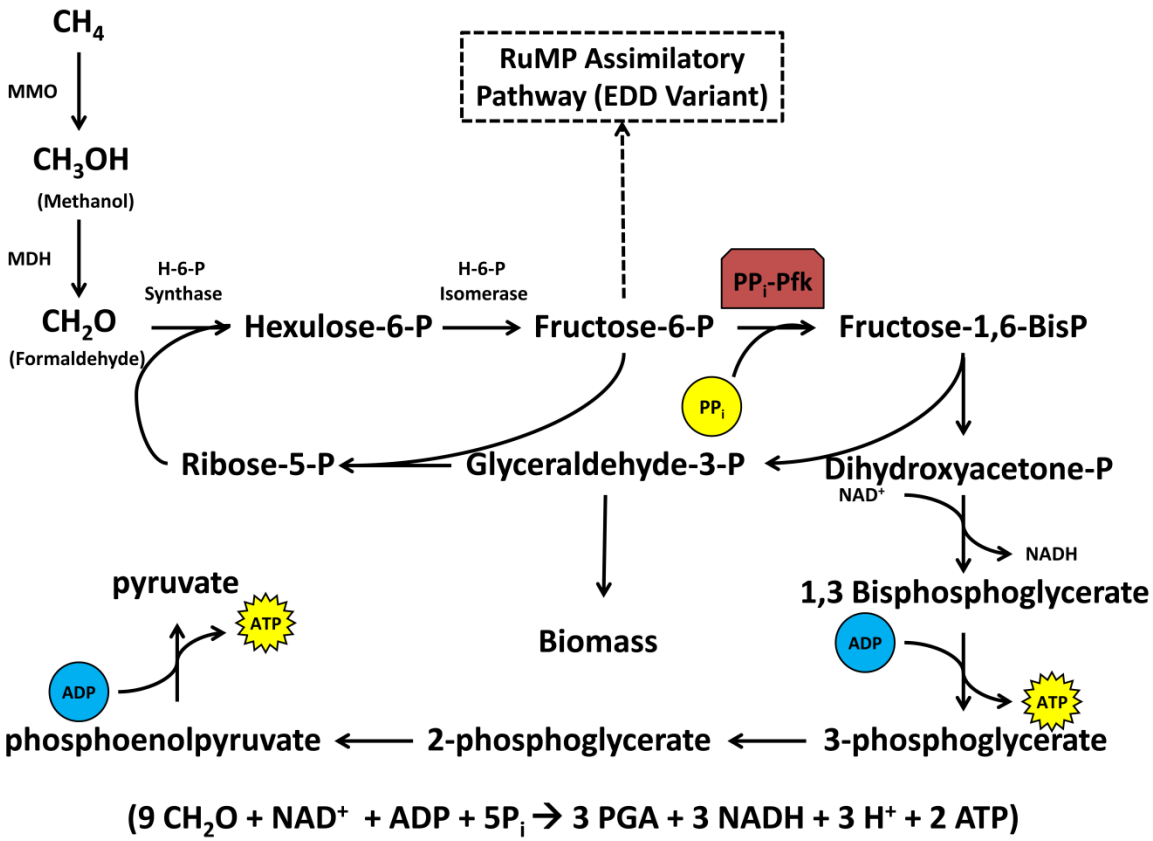

Figure 1.5 Pathway of the EMP-variant of the RuMP pathway in *M. alcaliphilum* str. 20Z adapted from Kalyuzhnaya, et al. 2013(66). MMO is methane monooxygenase, MDH is methanol dehydrogenase, P is phosphate, PPi is pyrophosphate, PPi-Pfk is the pyrophosphate-dependent phosphofructokinase, PGA is phosphoglycerate.

1.3.6 Nitrogen Assimilation by MOB

Nitrogen is an integral element in all life and MOB are no exception. MOB can assimilate nitrogen in two key ways: fixed nitrogen can be taken up by the cell and incorporated in into biomass or dinitrogen gas can be fixed from the atmosphere. Species in both the *Alpha-* and *Gammaproteobacteria* are capable of fixing nitrogen as well as veruccomicrobial methanotrophs (67, 68).

The relationship of MOB to ammonia is more complicated. This complication stems from the evolutionary relationship of ammonia monooxygenase (AMO) and MMO. AMO and MMO are homologous, sharing a common ancestor (69) (Fig. 1.1). As a result of the common ancestry of AMO and MMO the substrate specificity of AMO and MMO overlap. For example: AMO is capable of oxidizing methane and MMO is capable of oxidizing ammonia (70). MOB lack the ability to derive energy from the oxidation of ammonia by MMO and the oxidation of ammonia produces a toxic product, hydroxylamine (NH_2OH) (70). Hydroxylamine must be detoxified rapidly and many MOB possess detoxification pathways that transform hydroxylamine to nitric oxide (NO) and ultimately nitrous oxide (N_2O) (70). Nitrous oxide is a potent greenhouse gas more than 300 times as powerful as carbon dioxide in its global warming effect (1).

Excessive nitrogen has been found to both enhance and inhibit methanotrophy (70–72). The effect of ammonia may be beneficial if methane and other nutrients are in excess, allowing for elevated growth rates. However if methane is not in excess, high concentrations may be inhibitory. This results in an increase of greenhouse gases, nitrous oxide via hydroxylamine detoxification and escaping methane that cannot be oxidized by the inhibited methanotrophs (70).

1.4 Methane Biofilters: Function and Form

As the name suggests, methane biofilters rely on the biological oxidation of methane by assemblages of methanotrophic bacteria living within the filter. The biofilters are composed of soil which is spread over the methane source. All the methanotrophs that have been studied or detected in biofilters are aerobic. As a result, the most active methane oxidizing zone of the biofilter is generally the upper 30 to 40 cm with optimal rates of oxidation occurring at 15-20 cm of depth. This zone is where oxygen is plentiful enough for oxidation of methane to proceed (Figure 1.6) (71, 73).

1.4.1 Methane Supply into Biofilters

Biofilters can be supplied with methane gas in two ways. An active system pipes methane gas from the source to the biofilter in a controlled manner. The methane gas can be mixed with air in active systems and often the biofilters themselves are temperature and moisture controlled (71, 74) . Passive systems drive methane from the source into the biofilter by diffusion due to air pressure gradients between the gas source and the atmosphere (71, 75). Methane in passive systems can be piped to the biofilter or the biofilter can be integrated with the source forming a “window,” which is generally used in landfills (71). Windows, unlike other biofilters, are not self contained and are integrated with the methane source. When windows are used, porous material creates a pathway from the methane source in landfills to the biofilter (71). Windows have the advantage of being inexpensive when compared to other biofilter systems (71).

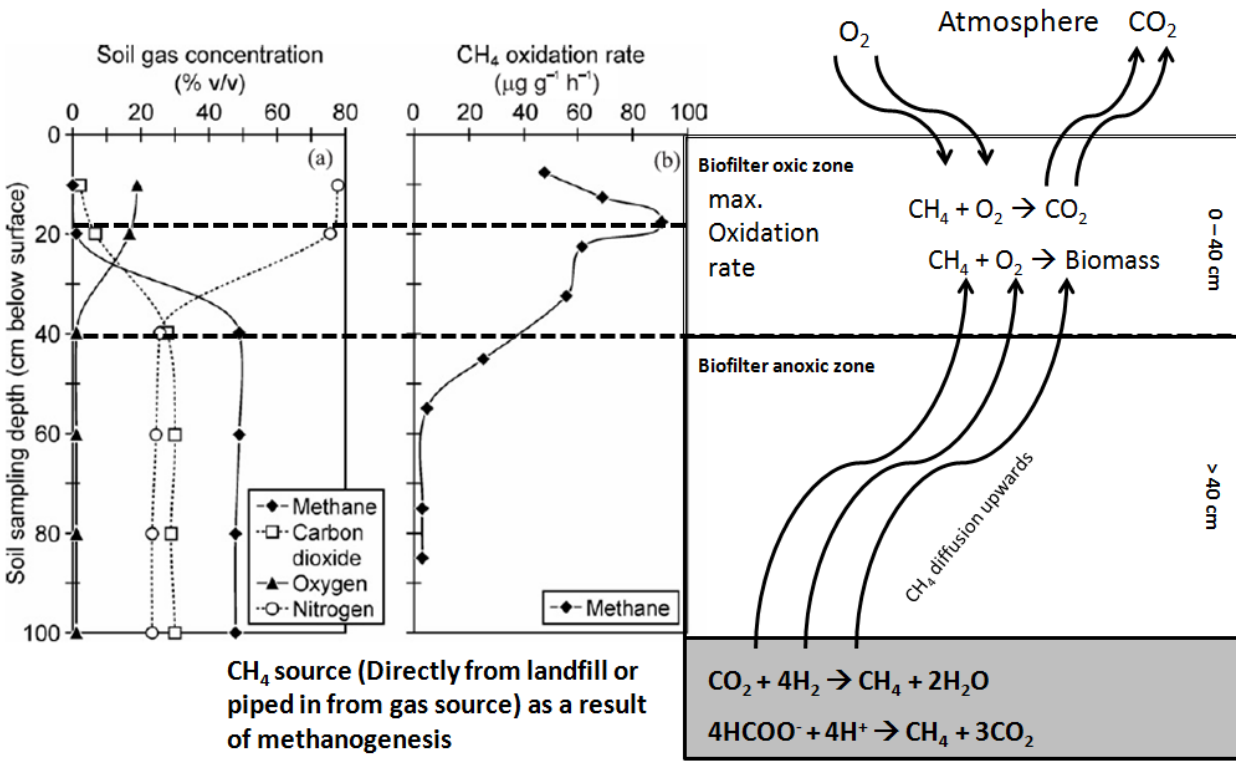

Figure 1.6 Diagram of upflowing biofilter accompanied by chemocline data
Diagram shows the concentrations of methane, carbon dioxide, oxygen, and nitrogen as well as methane oxidation rate with depth. Figure modified from Scheutz *et al*. 2009

1.4.2 Assessment of Biofilter Matrix Composition

The composition of the soil in biofilters can vary from organically poor material, sand for example, to organically rich material, such as compost. In general, biofilter material should be able to retain sufficient water to enable an optimal level of methane oxidation while maintaining a high permeability towards gas. The filter should be homogenous to prevent the leaking of feed gas from the source directly into the atmosphere. Lastly the filter should be resistant to microbial degradation (71). Settling, as a result of microbial degradation, can reduce gas permeability through the biofilter and therefore limit methane oxidation. Settling is of particular concern in methane biofilters primarily composed of organic material, such as compost (71).

Potential rates of methane oxidation cannot be compared easily between different soil types. There are a myriad of physical conditions that must be accounted for depending on the environment the biofilter soil is recovered from (71). Additionally, there is no standardized protocol to test the effectiveness of biofilter soils and differences in experimental conditions in the literature make it impossible to make direct comparisons between soil types. Because environmental conditions will vary from location to location, the best case scenario for the assessment of the best soil type to be implemented is to test each soil type under the environmental conditions (including seasonal variations) where the biofilter will be implemented.

Pawlowska *et al.* compared different biofilter materials under controlled conditions to determine the best materials for methane biofilter construction (76). The bed materials tested were Municipal Solid Waste (MSW) compost, horticultural

substrate, and composites utilizing the MSW with the addition of perlite (amorphous volcanic glass), calcium carbonate and either bentonite or zeolite (76). The ability of the biofilters to eliminate methane was tested over 6 months. During the 6 month test period, an increase in the capacity of all the biofilters to eliminate methane was observed (76).

Throughout the experiment, no significant difference was observed in the overall ability of the biofilter, composed of different materials, to eliminate methane (76). The only difference noted was the enhanced capacity of the composite containing zeolite to remove methane when only low concentrations of methane were applied to the methane biofilter (less than 3% methane) (76). The authors concluded that the bed material composition did not affect the ability of the biofilter to remove methane. At the end of the experiment, sewage sludge was applied to all the test biofilters and methane elimination was measured over the period of a week. The addition of the sludge greatly enhanced the ability of all the biofilters to remove methane, nearly two-fold. However, it is unclear if this enhancement was a result of the addition of exogenous MOB from the sewage sludge, augmenting the MOB community or if it was a result of nutrients being added to the system.

1.4.3 Aeration of Methane Biofilters

As mentioned previously, the biofilters in the study by Pawlowska et al. were aerated, exceeding recommended levels of oxygen of approximately 1.5% (71). High levels of oxygenation have been linked to the accumulation of EPS in the biofilter resulting in clogging (accumulation of biological substances, disrupting gas flow) and a

reduction of methane-oxidizing capacity of the biofilter. Despite the high levels of oxygen, no clogging was observed in the test biofilters. The authors concluded that this observation and the data on the kinetics of methane oxidation demonstrated that the biofilter community was mainly composed of *Alphaprotoeobacteria*. No definitive tests, such as molecular ecology experiments, were performed to corroborate this conclusion. Further work needs to be done to determine the dominant members of the MOB assemblage. This is a deficiency of many methane biofilter studies. The lack of a comprehensive analysis of microbial communities in methane biofilters hampers the ability of researchers to draw clear conclusions about how the microbiology of methane biofilters is affected by various physical conditions.

The linkage between over-aeration of biofilters and clogging of the biofilter bed with EPS has only been observed in actively vented biofilters (77, 78). The clogging effect is generally attributed to the presence of *Gammaproteobacteria* MOB which have been noted to generate greater amounts of EPS when compared to *Alphaproteobacteria* MOB (58). The accumulation of EPS is indicative of a nutrient imbalance in the biofilter, either as a result of excess carbon or the limiting amounts of other nutrients such as nitrogen (79).

Long term studies of soil type influencing the efficiency of methane removal are also largely absent from the literature with most studies running for less than one year (71). Though long term effects and environmental effects such as seasonal changes are understudied, some broad conclusions can be drawn about the influence of physico-chemical factors on methane oxidation in methane biofilters, chiefly: temperature, soil moisture, and inorganic nitrogen content.

1.4.4 Temperature and Moisture Effects on Methane Biofilters

Temperature has been found to be one of the most important parameters affecting the oxidation of methane in biofilters. While methanotrophs have been found to have varying optimal growth temperatures, methane biofilters have on average been found to have optimal rates of methane oxidation between 25^{o}C and 35^{o}C (79). Different temperatures affect which MOB are dominant in the methane biofilter. Community composition monitoring demonstrated that *Gammaproteobacteria* tend to dominate the MOB assemblages at lower temperatures (10^{o}C) (80). *Alphaproteobacteria* tended to dominate assemblages at warmer temperatures (20^{o}C) (80). Temperature poses significant challenges for biofilters that are utilized in variable climate areas. Often the only solution is to control temperature of the biofilter, an energy intensive process.

Soil moisture affects the availability of gaseous substrates in biofilters. When water saturation of a biofilter (measured as a ratio of water volume to void volume in the soil, v/v) reaches 85% v/v, air filled spaces in the soil disconnect, impeding the diffusion of gas into the soil (79). The impediment of diffusion is a result of the relatively slower rate of gas diffusion through aqueous phase compared to gas phase. Slower rates of diffusion limit both oxygen and methane leading to a reduction in the rates of methane oxidation. Very high levels of soil moisture can result in the stimulation of methanogenesis as a result of expanded anaerobic zones within the biofilter soil. In addition, high levels of moisture can result in the lateral migration of the flow of gas along the relatively dry path within the biofilter (71). Lateral migration of methane gas from a landfill can be extremely dangerous; for example, lateral migration of methane

from a landfill in Denmark resulted in a fatal explosion in a home near the landfill site (79).

Typically, optimal rates of methane oxidation occur with moisture levels of approximately 20% v/v (79). Moisture levels below 5% v/v tend to inhibit methane oxidation. Low soil moisture levels can also result in fissures forming on the surface of the biofilter. These fissures introduce heterogeneity within the biofilter, creating passages for methane and other gases to escape into the atmosphere. The escaping methane from these fissures is a significant contributor to the total methane flux into the atmosphere from landfill sites.

Hettiarachchi *et al.* tested the effect of environmental conditions, in particular ambient temperatures and precipitation, on the capacity of methane biofilters to oxidize methane (81). The optimal temperature of the methane biofilter was found to be around 20 – 36^{o}C, consistent with previous literature on optimal temperatures for biofilters (81). Diurnal occurrences, such as temperature and humidity changes, did not appear to affect the methane oxidizing capacity of the biofilter (81). Temperature change lasting over several days also did not seem to affect the effectiveness of the methane biofilter. Several days of rain fall, resulting in elevated moisture levels in the biofilter, did have a negative effect on the efficiency of the methane biofilter (81). Three to five days after the rainfall event, the efficiency of the biofilter returned to normal, reaching nominal soil moisture percentages (81).

Seasonal effects were also tested. Ambient temperatures of -20^{o}C resulted in a rapid decline of the efficiency of the methane biofilter. Warmer ambient temperatures (-

10°C and 0°C) slowly decreased the efficiency of the methane biofilter. Regardless of whether the temperature decline was rapid or slow, once the biofilter temperature reached 5°C, it ceased to function effectively (81).

1.4.5 Nitrogen Effects on Methane Biofilters

Inorganic nitrogen content is another important factor moderating methane oxidation rates in biofilters as the soils tend to be N-limited (71). In literature, amendments of nitrogen to soil are generally either in the form of ammonia (NH_3) or nitrate (NO_3^-). Nitrate amendments do not inhibit methanotrophy unless very high amounts of nitrate are added to an environment (71, 82). The response of methanotrophs to ammonia amendments in literature is varied and sometimes contradictory. Some studies indicate a decrease or complete inhibition of soil methane oxidizing ability with ammonia amendment (72, 73, 83–85). Other studies show and enhancement of methane oxidizing capabilities with the addition of ammonia (86, 87). Both results can make sense when the physiology of MOB is taken into account.

As mentioned previously, the methane monooxygenase is evolutionarily related to the ammonia monooxygenase and MOB are capable of oxidizing ammonia, but are not able to grow using it as an energy source. Ammonia can compete with methane for the MMO active site, inhibiting methane oxidation and therefore, MOB growth. Another aspect of inhibition by ammonia is the production of toxic products as a result of ammonia oxidation to hydroxylamine (NH_2OH) (see physiology section). A potential consequence of over-fertilization with ammonia may be the production of nitrous oxide, an even more powerful greenhouse gas than carbon dioxide (88).

One possible way to avoid excess nitrous oxide emission is discussed by Im *et*

al. (88). In this study the maximization of methane oxidation with ammonia amendments without nitrous oxide production was achieved by adding phenylacetylene to the soil. Phenylacetylene is a selective inhibitor of AMO, sMMO, and pMMO (45). Combined with dryer soils (5% v/v), a substantial reduction of nitrous oxide was observed while maximizing methane oxidation (45, 88).

What about methane oxidation enhancement in the presence of ammonia fertilization? One of the simplest explanations, though often overlooked in literature, for the enhancement of methane oxidation rates with ammonia amendments is that nitrogen is limiting in the environment where ammonia is added. A second explanation is a switch from nitrogen fixation, an energetically expensive process, to ammonia uptake in *Alphaproteobacteria*. This switch frees up more energy for growth, thus enhancing methane oxidation rates.

Another indirect reason for the enhancement of methane oxidation with ammonia fertilization is the stimulation of plant growth (71). Plants have been found to regulate the soil moisture levels in biofilters enhancing methanotrophy. In addition, plants secreting plant root exudates may create more favourable conditions, though these conditions are not well understood (71, 84).

1.4.6 Volatile Sulfur Compound Effects on Methane Biofilters

Another potential inhibitor of MOB in biofilters is volatile sulfur compounds (VSCs) (89). Sulfur molecules such as methanethiol (CH_3SH) and carbon disulphide (CS_2) occur naturally in systems where methane is generated, for example in landfills (89). The VSCs form when protein breaks down and are a significant contributor to

odour in landfill sites and waste water treatment plants (89). The VSCs are especially problematic in newer landfill sites and act to slow the establishment of methanotrophs in biofilters (89). VSCs also seem to select against *Gammaproteobacteria* in the methanotrophic assemblage, though it is unclear why (89).

1.4.7 Phosphate and Metal Requirements in Methane Biofilters

Other studies have looked at the importance of potential key nutrients in biofilter soils. Nikiema *et al.* studied the effect of phosphate, potassium, copper, and other trace metals on rates of methane oxidation in methane biofilters (90). Nikiema *et al.* found that amendments of copper, potassium, and other trace metals had no significant effect on the rate of methane oxidation in methane biofilters (90). The lack of effect on methane oxidation capacity indicates that the metals tested are not limiting to the MOB present in the filter. This means that either the nutrients are present in sufficient amounts or that the MOB present do not require the metals. The authors suggests that trace metals and other nutrients are likely present in sufficient amounts in ordinary tap water, therefore additional amendments are likely redundant (90). The results, especially for copper, are still surprising as studies on methanotrophic assemblages in rice paddy soil and compost MOB enrichments have observed an increase in methanotrophic activity with the addition of copper (91, 92).

Conversely, amendments of phosphate to the biofilter enhanced the ability of the biofilter to eliminate methane (90). The phosphate amendment also shortened the period of time that the methane biofilter takes to reach optimal levels of methane oxidation. Phosphate addition also increased the rate of bioclogging of the methane

biofilter. Nikiema *et al.* noted that a smaller amount of phosphate should be added if the methane biofilter is to be used over a long period of time (90).

1.5 The Goldbar Biofilter

This project studied the microbiology of a methane biofilter in partnership with the Edmonton Waste Management Centre of Excellence at the Goldbar Wastewater Treatment Plant and the Buchanan Lab at the University of Alberta, faculty of Engineering. This project centred on two pilot scale bioreactors that were being tested to generate biogas from a variety of organic industrial wastes. Because of the test conditions that the bioreactors were being subjected to it was expected that the methane output of these two pilot scale reactors would be highly variable. Because of this variability, flaring the output methane gas was concluded to be a poor choice in ensuring that the methane was not released into the air, for environmental, health and safety concerns. The approach of using a methane biofilter was concluded as being the most effective choice in dealing with the output methane as well as the most cost effective.

The pilot scale reactors and bioreactors were set up according to Figure 1.7**.** Methane produced by the reactors was piped initially towards a chemical hydrogen sulfide scrubber and then subsequently piped into the base of the methane biofilter. The movement of gas from the bioreactors into the biofilter was passive with back pressure building up only at peak gas production times. Upon entering the biofilter the feed pipes split into three pipes that ran along the base of the biofilter. These pipes were perforated along the entire length of the biofilter allowing gas from the bioreactor

to diffuse into the biofilter pile, which consisted of municipal compost and woodchips. Methanotrophs within the biofilter oxidized the methane to carbon dioxide or incorporated the carbon into their biomass.

From April of 2011 to January of 2012, gas fluxing from the biofilter and the biofilter medium was sampled on a weekly basis. Gas samples were analyzed for the presence of methane to test if the filter was effective at preventing in part or entirely the release of methane into the atmosphere. MBF medium samples were collected from the surface of the biofilter for the characterization of the general bacterial and methanotrophic communities. This project assessed the species richness of the bacterial and MOB communities residing in the biofilter using restriction fragment length polymorphism (RFLP) and terminal restriction fragment length polymorphism (TRFLP) of PCR-amplified gene sequences. The relative abundance of methanotrophs in the biofilter was determined using quantitative PCR (qPCR) using a well characterized genetic marker for MOB, the gene *pmoA* which encodes for a subunit of the pMMO. A second marker was also used, the recently discovered *pxmA* gene (see section1.3.1).

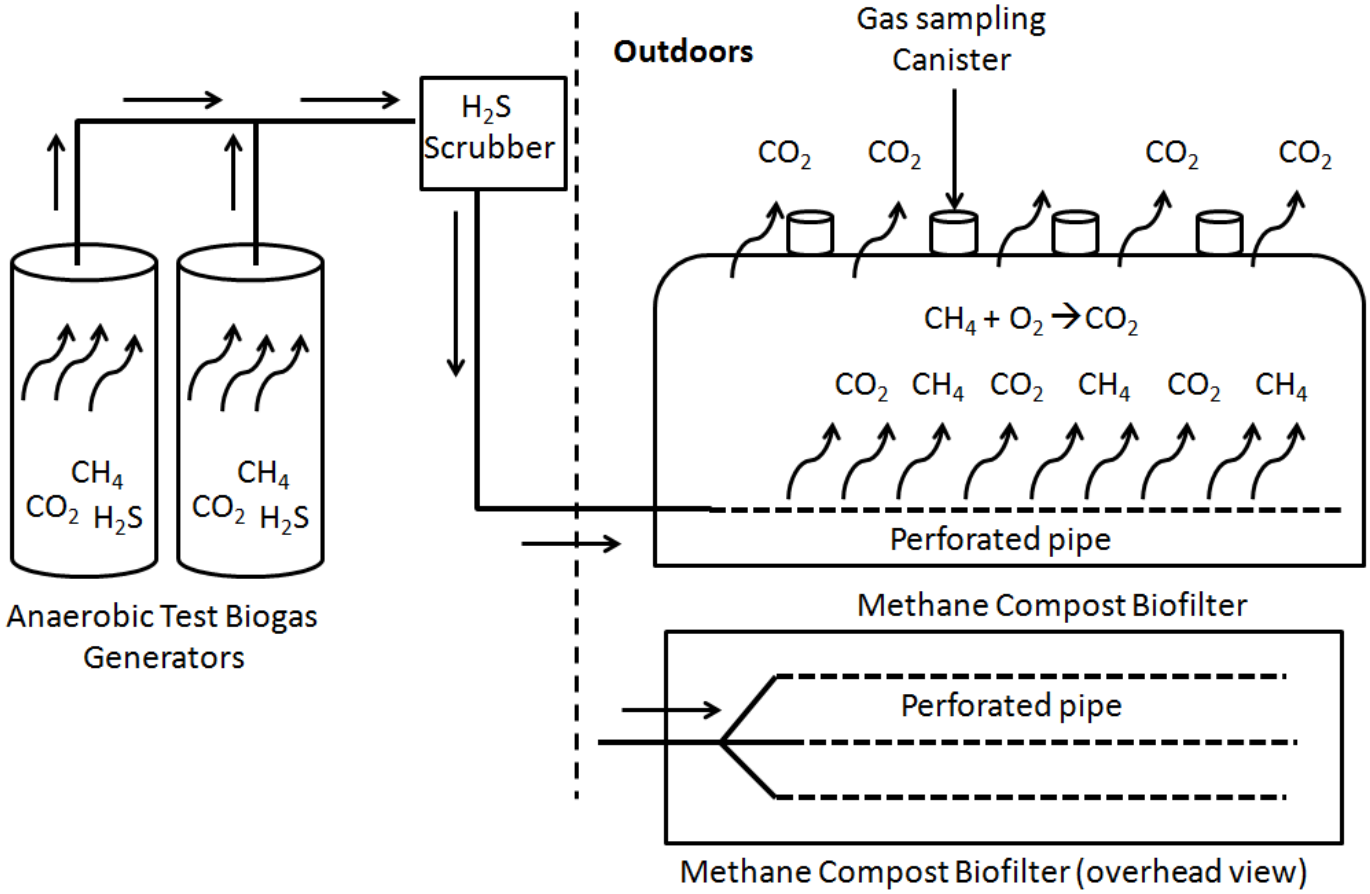

Figure 1.7 Schematic of the pilot scale biogas generators and methane biofilter at Goldbar.

Gas from the biogas generator first passes through a hydrogen sulfide scrubber before being piped to the biofilter. The feed pipe splits into three perforated pipes (indicated by dashed lines) upon entering the biofilter. The perforated pipes allow the gas to diffuse into the biofilter. Methane is oxidized by methanotrophs to carbon dioxide. Gas sampling points are located across the length of the biofilter

1.6 Objectives and Hypotheses

The goals of this experiment were to determine how the diversity and abundance of the biofilter community varied over time and over changing levels of methane input. Comparisons were made between methane input, the age of the biofilter and *pmoA* diversity and abundance to determine if a correlation existed.

It was hypothesized that the MOB community changes in response to the variable methane input into the biofilter. It was predicted that a lack of methane input would result in a decline in the MOB population while the presence of methane would increase the numbers of MOB present. With regard the diversity of the MOB community, it was expected that the diversity of the MOB community would change with methane input and also due to aging of the biofilter itself.

2.0 Methods

2.1 MBF medium and gas sampling

2.1.1 MBF medium sampling from the methane biofilter

MBF Medium samples from the MBF were collected from March 30th to December 1st of 2011 at the methane biofilter at the Goldbar Waste Water Treatment Facility in Edmonton, Alberta, Canada. Samples were collected from four different locations along the length of the biofilter (Figure 2.1). From each location on the MBF four samples of the first 10-20 cm of top MBF medium, the predicted optimal region in the biofilter for MOB (71, 73), were collected and then sieved through a 2mm sieve into an unused autoclave bag (see table 2.1 for samples collected). The sieved MBF medium was then collected into 50 ml Falcon tubes and transported back to the lab and

stored at -80^{o}C until processing. During the winter months some sample locations were not sampled due to freezing of the biofilter MBF medium. Soil to be used for the enrichment of MOB was left unsieved and was returned to the lab for further tests (see section 2.10).

2.1.2 Gas sampling at the methane biofilter

Gas samples were collected when the test bioreactors were active (see Table 2.1 for samples taken). To collect flux gas from the surface of the biofilter, empty aluminum coffee cans with a butyl septum glued onto the bottom were placed along the length of the biofilter top down, creating a closed-top chamber. The cans were placed into the biofilter soil to a depth of approximately 5-10 cm. To collect flux gas, a 60 ml syringe was inserted through the septum and 120 ml of gas was collected from the chamber and stored in a gas sampling bag for later analysis. Samples were taken in duplicate, but due to limitations of the number sample gas bags available not all sampling locations were sampled on the same days. A control sample of the atmospheric gas was also taken at the site.

Feed gas emitted from the bioreactors was sampled from a valve downstream of a chemical hydrogen sulphide scrubber. Sampling was performed by placing a nitrile glove over the valve and securing it with a twist tie. The valve was then opened and the feed gas was allowed to inflate the glove. A 60 ml syringe and needle were then used to withdraw 120 ml of volume from the nitrile glove and into a gas sampling bag. All analyses of the gas samples were performed on the day of sampling to ensure accuracy (section 2.7).

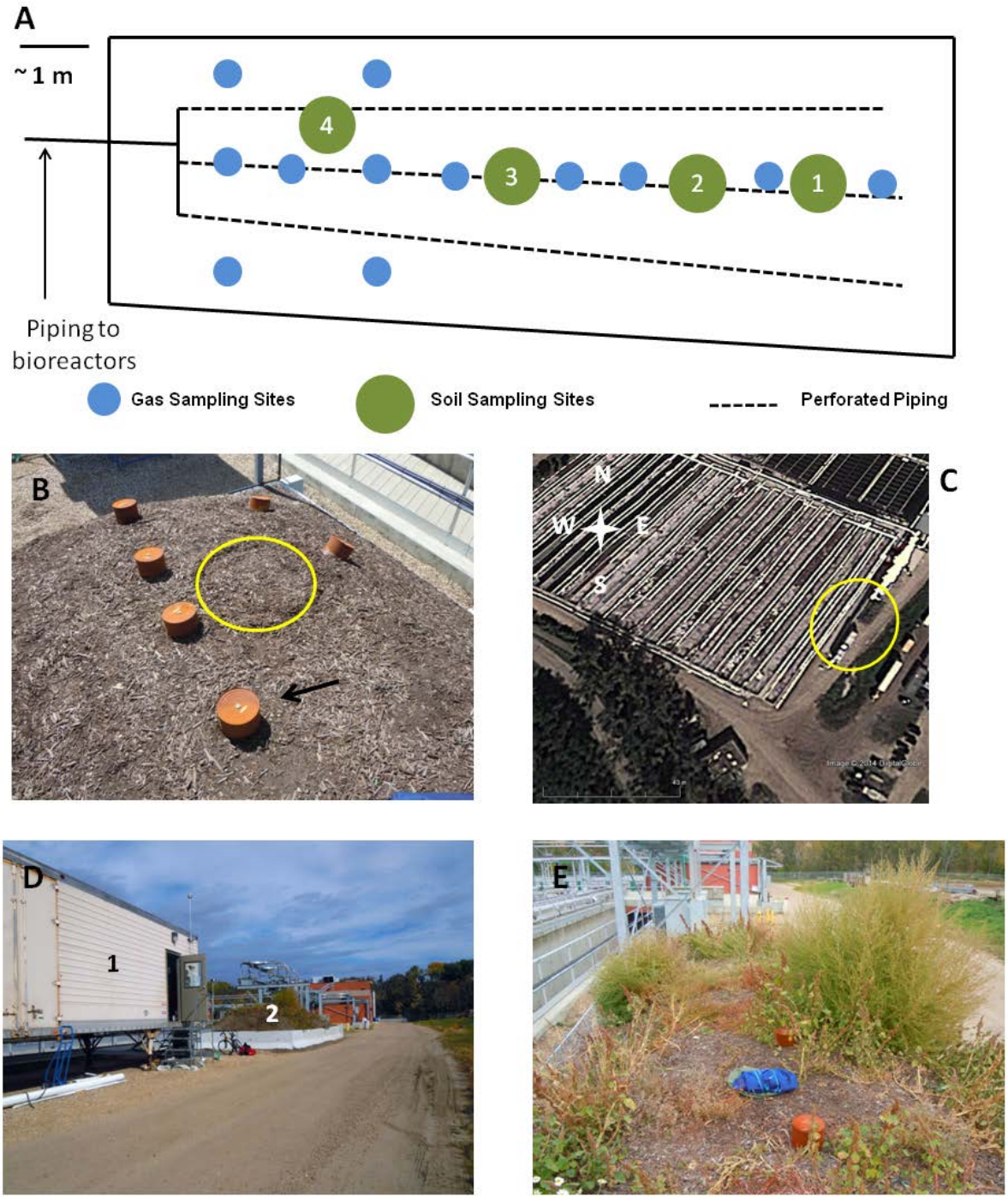

Fig 2.1 The methane biofilter located at the Goldbar Waste Water Treatment Plant
A) Illustration of the biofilter layout with sampling sites. Methane gas was passively fed into the biofilter from the digesters. **B)** Photo from the biofilter showing the closed-top chamber (indicated by the arrow) and one of the sampling zones (outlined in yellow). **C)** Satellite image (Google) of the methane biofilter and digester trailer (circled in yellow) at the Goldbar Waste Water Treatment Plant (August, 2010). **D)** Photo of the trailer containing the digester (1) and the methane biofilter (2). **E)** Photo demonstrating plant growth on the biofilter during the summer months.

Table 2.1 Soil samples collected during the lifespan of the methane biofilter
Sample composites are shown in the first column. Gas samples were taken on the same dates when biogas was being produced.

Composite number (GB)	Sample Site	Sampling Date
A	1 2	2011-03-30
1	1 2 3 4	2011-05-12
2	1 2 3 4	2011-05-17
3	1 2 3 4	2011-05-27
4	1 2 3 4	2011-06-01
5	1 2 3 4	2011-06-09
6	1 2 3 4	2011-06-23
7	1 2 3 4	2011-06-28
8	1 2 3 4	2011-07-08
9	1 2 3 4	2011-07-14
10	1 2 3 4	2011-07-19
11	1 2 3 4	2011-07-28
12	1 2 3 4	2011-08-04
13	1 2 3 4	2011-08-11
14	1 2 3 4	2011-08-18
15	1 2 3 4	2011-08-25
16	1 2 3 4	2011-08-30
17	1 2 3 4	2011-09-13
18	1 2 3 4	2011-09-22
19	1 2 3 4	2011-09-27
20	1 2 3 4	2011-10-13
21	1 2 3 4	2011-10-20
22	1 2 3 4	2011-11-02
23	1 2 3 4	2011-11-24
24	2 3	2011-12-01

2.2 Nucleic Acid Extractions

2.2.1 DNA extraction from the biofilter compost: Griffith Extraction

The DNA extraction protocol used for the MBF medium extraction is based on the protocol by Griffith et al., 2000 (93). One-half gram of soil from each sample location and date was weighed into a 2 ml screw-top tube containing ceramic spheres, 0.1mm silica spheres, and one 4 mm sphere (Lysing Matrix E from MP Biomedicals). To the bead-soil mixture 500 µl of a 5% w/v Cetyl trimethylammonium bromide (CTAB) - 120 mM phosphate buffer solution was added. Next, 500 µl of a 25:24:1, phenol: chloroform: isoamyl alcohol (IAA) (pH 8.0) solution was added into the 2 ml tube. Tubes were sealed and then placed in a bead beater (Precellys® 24, Bertin Technologies) and run at speed setting 5,000 for 20 seconds, placed on ice, then run again at the same speed for an additional 20 seconds and then placed on ice.

After bead beating the 2 ml tubes were spun down at 16,000 x g for 5 min at room temperature (RT). The aqueous phase was removed from the tube by pipetting and was placed into a new 1.5 ml centrifuge tube. To the 1.5 ml tube containing the aqueous phase, an additional 500 µl of 24:1 chloroform: IAA was added to remove residual phenol. The mixture was mixed by inversion and then centrifuged at 16,000 x g for 5 min at RT. The aqueous phase was transferred to a new 1.5 ml tube for further steps.

To the transferred aqueous phase, 2 volumes of 30% PEG 8000 (Fisher Scientific) were added. The PEG-aqueous phase was vortexed to mix solutions and then incubated overnight at 4^{o}C to precipitate the DNA. After incubation the precipitated

DNA was spun down at 16,000 x g for 20 min at room temperature (RT). The supernatant was poured off and residual amounts were carefully removed with a micropipetter. The DNA pellet was resuspended in 1,000 µl of ice cold 70% ethanol, mixed by vortexing, and then centrifuged at 16,000 x g for 20 min at RT. Supernatant was decanted and then residual amounts were removed by micropipetting. The pellet was placed on a 55^{o}C heating block for 2 min to remove any remaining ethanol. The pellet was resuspended in 50 µl of nuclease-free water. The extracted DNA was inspected by agarose gel electrophoresis (see section 2.4.1) and was stored at -80^{o}C with working stocks stored at -20^{o}C. Extracted DNA from each sample site was composited based on date (see Table 2.1).

2.2.2 Additional sephadex G200 purification of extracted DNA

For some downstream applications, such as qPCR and terminal-restriction fragment length polymorphism (T-RFLP) (see section 2.6), additional purification of the extracted DNA was required to reduce PCR inhibition. The purification of the DNA by Sephadex G200 was performed as per Miller et al., 1999 (94). One gram of Sephadex G200 was hydrated and washed 10 times with a high salt TE reconstitution buffer (10 mM Tris-HCL, 1mM EDTA, 100 mM NaCl at pH 8) and then autoclaved. Autoclaved cotton was used to line the bottom of a 1 ml syringe, occupying 0.1 ml of space in the syringe. The syringe was then filled with the saturated sephadex G200 - TE buffer mix. The filled syringe was placed into a 15-ml Falcon tube and then spun at 1,100 x g for 15 min at 4^{o}C to remove excess buffer. After spinning, additional Sephadex G200 - TE buffer was added to the syringe and once again was centrifuged at 1,100 x g for 15 min at 4^{o}C. This process was repeated until the syringe was filled to the 1 ml mark with

sephadex G200 beads and then the syringes were transferred to new sterile 15 ml Falcon tubes.

High salt TE buffer was added to the DNA samples requiring additional purification. The buffer was added directly to the extracted DNA to a total buffer and sample volume of 300 µl. One hundred microlitres of sample was added to the column and spun at 1,100 x g for 15 min. Sample application to the column was repeated until all 300 µl of volume had been run through the column. Following this an ethanol based DNA precipitation was performed to concentrate the eluted DNA.

2.2.3 Ethanol precipitation of DNA

One-tenth the volume of 3M sodium acetate, pH 5.2 was added to the eluted DNA. Next, 2.5 volumes of 100% ethanol (-20^{o}C) was added to the eluent to precipitate the DNA and incubated at -80^{o}C for 30 min and then centrifuged at 16,000 x g for 20 min at 4^{o}C. The supernatant was removed by pipetting and 1000 µl of 70% ethanol was added to wash the pellet. The mixture was centrifuged again for 5 minutes at 4^{o}C and the supernatant was removed and the pellet was dried at 55^{o}C for 2 minutes to remove residual ethanol. The DNA was resuspended in 50 µl nuclease- free water. The concentration of recovered DNA was measured by nanodrop (Thermoscientific) and Qubit analysis (Life Technologies) (see section 2.8 for method). The purified DNA was stored at -20^{o}C.

2.2.4 Gel purification of *pmoA* amplicon using QiaQuick Gel Extraction Kit (Qiagen)

This protocol was performed as per manufacturer instructions. The *pmoA* amplicon to be purified was loaded onto the agarose gel, run, and stained as per section 2.4.1. On a UV transilluminator the 500 bp *pmoA* band was identified and excised from the gel using a razor. As much excess agarose was trimmed away from the band as possible and then the piece of agarose containing the band was place into a 1.5 ml microcentrifuge tube and weighed. Three volumes of buffer QG (v/w) (guanidine thiocyanate) was added to the gel slice in the tube and then incubated at 50^{o}C for 10 min with occasional vortexing.

One gel volume of 100% isopropanol was added to the mixture and vortexed. The resulting DNA, buffer QG, isopropanol mixture was loaded onto a silica spin column and centrifuged at 10,000 x g for 1 minute at RT. The flow-through was discarded and 0.75 ml of buffer PE was added to the wash the column. The tube was centrifuged again at 17,900 x g for 1 minute at RT and the flow-through was discarded. A second spin was performed after discarding the flow- through to remove residual buffer PE. The column was removed from the catch tube and place in a nuclease- free 1.5 ml microcentrifuge tube for DNA elution. The DNA was eluted by adding 50 µl of nuclease free water to the column and centrifuging using the above conditions. DNA was quantified using Nanodrop and/or Qubit (see section 2.8). The purified DNA was stored at -20^{o}C until needed.

2.2.5 Purification of amplicon using Qiaquick column purification kit (Qiagen)

For amplicon purification, 150 µl of amplicon was collected for the purification kit. Five volumes of the proprietary buffer PB was added to the amplicon. Ten microlitres of a 3M sodium acetate pH 5.2 was added to lower pH for the purification for binding to the silica column. The buffer PB, amplicon mixture was applied to the silica binding column and the column was centrifuged at 17,900 x g for 1 min at RT. The flow-through was discarded and 0.75 ml of buffer PE was applied to wash the column. The column was centrifuged at 17,900 x g for 1 min at RT and the flow-through was discarded. A second centrifugation was performed to remove residual buffer PE. The column was transferred to a nuclease-free 1.5 ml microcentrifuge tube. Fifty microlitres of nuclease-free water were added to the column and then was centrifuged again at 10,000 x g for 1 min at RT. DNA was quantified using Nanodrop and/or Qubit analysis (see section 2.8). The purified DNA was stored at -20^{o}C.

2.2.6 Genomic DNA extraction from cultivated cells

This protocol was adapted from the Joint Genome Institute (available at http://jgi.doe.gov/wp-content/uploads/2014/02/JGI-Bacterial-DNA-isolation-CTAB-Protocol-2012.pdf). Cells from the culture to be extracted were pelleted prior to extraction (10,000 rpm, 5 min). The cell pellet was resuspended in TE buffer (10 mM Tris, 1 mM EDTA, pH 8) to an OD_{600} of 1. lysozyme (20 µl, 100 mg/ml) was added to 740 µl of the resuspended cells and the mixture was incubated at RT. After 5 minutes, SDS (10%, 40 µl) was added followed by proteinase K (8 µl, 10 mg/ml) and incubated at 37^{o}C for 1 hr.

Following the incubation, NaCl (5 M, 100 µl) and CTAB/NaCl (0.7M NaCl, 10% CTAB; 100 µl) heated to 65^{o}C was added. After 10 min of incubation at 65^{o}C, 0.5 ml of phenol:chloroform:IAA (25:24:1) was mixed in and then the mixture was centrifuged (16,000 x g, 10 minutes, RT). After centrifugation the aqueous phase was transferred to a sterile 1.5 ml microcentrifuge tube and 24:1 chloroform:IAA was added. The mixture was centrifuged again (16,000 x g, 10 minutes) and the aqueous phase was transferred to a sterile 1.5 ml tube. Isopropanol (0.6 volumes) was added to the transferred aqueous phase and the tube was incubated at 4^{o}C overnight.

After incubation the precipitated DNA was centrifuged at 16,000 x g for 15 min. The supernatant was decanted after centrifugation and the DNA pellet was washed with 70% ethanol (1000 µl) and centrifuged again at the same speed for 5 min. The supernatant was decanted and the DNA pellet was dried on a heating block at 55^{o}C for 5 min to remove residual ethanol. The DNA was resuspended in nuclease-free water (50 µL) and the quality of the DNA was checked on an agarose gel. The extracted DNA was quantified by Nanodrop analysis (section 2.8).

2.3 Polymerase chain reaction protocols

All PCR reactions were run on a Veriti® thermal cycler from Life Technologies™. Unless otherwise indicated dNTPs were purchased from Fermentas Life Sciences, primers from Integrated DNA Technologies, and 10X amplification buffer (500 mM KCl, 15 mM $MgCl_2$, 100 mM Tris-Cl) was prepared as per Sambrook and Russell (2001). Primer sequences with references are in Table 2. The amplicons were checked on an

agarose gel to determine if amplification had proceeded correctly and if there was any DNA contamination present (see section 2.4.1).

2.3.1 Amplification of the bacterial 16S rRNA gene for DGGE

Amplification of the 16S rRNA gene for DGGE was performed using the primers 518R and 341F, where primer 341F had a GC clamp (see Table 2.2 for sequence and reference). The GC clamp prevents complete separation of the amplicon when it run on the subsequent denaturing gradient gel (see section 2.4.2). Each 50 µl reaction consisted of 5 µl of 10X PCR amplification buffer, 0.1 mM dNTPs, 0.1 µM primer 518R, 0.1 µM of GC-clamped primer 341F, 5 U of taq polymerase, and 2 µl of $1/10^{th}$ diluted DNA template from the extracted Goldbar MBF medium samples. Reactions were prepared with a positive control consisting of bacterial genomic DNA and a negative control with no template added to the reaction. The PCR cycle began with an initial denaturation step at 95^{o}C for 3 min followed by 9 cycles of touch down PCR (94^{o}C for 30 sec, 65^{o}C for 30 sec -1^{o}C per cycle, 72^{o}C for 30 sec). The touchdown cycles were followed by 30 cycles at a static annealing temperature (94^{o}C for 0:30 minute, 55^{o}C for 0:30 minute, 72^{o}C for 0:30 minute) and final extension step at 72^{o}C for 10 min.

2.3.2 Amplification of the bacterial 16S rRNA gene for RFLP

Amplification of the 16S rRNA gene for 16S RFLP analysis of the MOB enrichment GB074 was performed using the primers 1492R and 27F (see Table 2.2 for sequence and reference). Each 25 µl reaction consisted of 2.5 µl of 10X PCR amplification buffer, 0.1 mM dNTPs, 0.1 µM primer 1492R, 0.1 µM of 27F, 5 U of taq polymerase, and 2 µl of DNA template from the extracted GB074 enrichment. Reactions

were prepared with a positive control consisting of bacterial genomic DNA and a negative control with no template added to the reaction. The PCR cycle began with an initial denaturation step at 95^{o}C for 3 min followed by 39 cycles of amplification (94^{o}C for 30 sec, 55^{o}C for 30 sec, 72^{o}C for 30 sec) and then a final extension step of 72^{o}C for 10 minutes.

2.3.3 Amplification of the bacterial 16S rRNA gene for T-RFLP

Amplification of the 16S rRNA gene for 16S T-RFLP analysis (section 2.6) was performed using the primers 907R and 27F^{FAM}. Each 50 µl reaction consisted of 5 µl of 10X PCR amplification buffer, 0.2 mM dNTPs, 0.2 µM primer 907R, 0.2 µM of 27F^{FAM} (labelled with the fluorescent tag, 6-carboxyfluorescein, FAM, on the 5' end), 2.5 U of taq polymerase, 0.1 mg/ml BSA, and 1 µl of DNA template (10 ng). Reactions were prepared with a positive control consisting of bacterial genomic DNA and a negative control with no template added to the reaction. The PCR cycle began with an initial denaturation step at 95^{o}C for 5 min followed by 25 cycles of amplification (95^{o}C for 30 sec, 57^{o}C for 30 sec, 72^{o}C for 1 min) and then a final extension step of 72^{o}C for 10 min.

2.3.4 Amplification of the *pmoA* gene for RFLP

Amplification of the *pmoA* for RFLP analysis (section 2.5) was performed using the primers mb661 and A189F which target the *Gamma-* and *Alphaproteobacteria* MOB (see Table 2.2 for reference and sequence). Each 25 µl reaction consisted of 2.5 µl of 10X PCR amplification buffer, 0.1 mM dNTPs, 0.1 µM primer mb661, 0.1 µM of A189F, 5 U of Taq polymerase, 0.1 mg/ml BSA, and 2 µl of DNA template. Reactions were prepared with a positive control consisting of MOB genomic DNA and a negative control

with no template added to the reaction. The PCR cycle began with an initial denaturation step at 95^{o}C for 5 min followed by 40 cycles of amplification (95^{o}C for 30 sec, 55^{o}C for 30 sec, 72^{o}C for 5 min) and then a final extension step of 72^{o}C for 5 minutes.

2.3.5 Amplification of the *pmoA* gene for T-RFLP

Amplification of *pmoA* for T-RFLP analysis was performed using the primers mb661^{TET} and A189F (see Table 2.2 for reference and sequence). Each 50 µl reaction consisted of 25 µl of 2X AccuStart II Tough master mix (Quanta Biosciences), 0.2 µM primer mb661^{TET} (labelled with the fluorescent dye 5-tetraschlorofluorescein, TET, on the 5' end), 0.2 µM of A189F, and 1 µl of DNA template. Reactions were prepared with a positive control consisting of MOB genomic DNA and a negative control with no template added to the reaction. The PCR cycle began with an initial denaturation step at 95^{o}C for 5 min followed by 10 cycles of touch-up amplification where the annealing temperature increase by 1^{o}C per cycle starting from 60^{o}C (95^{o}C for 30 sec, 60^{o}C+1^{o}C/cycle for 30 sec, 72^{o}C for 30 sec). This was followed by an additional 25 cycles (95^{o}C for 30 sec, 58^{o}C for 30 sec, 72^{o}C for 1 min) and then a final extension step of 72^{o}C for 5 minutes. Touch-up PCR was used because it was found to give the most specific and plentiful PCR product.

2.3.6 Amplification of the insert from the Pcr2.1 plasmid

Amplification of insert as part of the clone library step (see section 2.5.1) for RFLP analysis was performed using the primers M13R and M13F (see Table 2.2 for reference and sequence). Each 50 µl reaction consisted of 5 µl of 10X PCR

amplification buffer, 0.1 mM dNTPs, 0.1 µM primer M13R, 0.1 µM of M13F, 5 U of Taq polymerase, and a small amount of cell mass from a colony or a cell suspension in low TE buffer. Reactions were prepared with a negative control with no template added to the reaction. The PCR cycle began with an initial denaturation step at 94^{o}C for 4 min followed by 35 cycles of amplification (94^{o}C for 1 min, 55^{o}C for 1 min, 72^{o}C for 1 min) and then a final extension step of 72^{o}C for 10 minutes.

2.3.7 Sanger dideoxy sequencing using BigDye reaction mix

Sequencing of clones from the RFLP analysis was conducted using Sanger dideoxy sequencing using the protocol supplied by the Molecular Biology Services Unit (MBSU). The reaction contained 2 µl of BigDye (Life Technologies) v3.1 premix (prepared by the MBSU), 3µl of 5x sequencing buffer, 1 pmol of primer, and 100 ng of PCR product. The sequencing cycle started with 30 sec at 96^{o}C followed by 25 sequencing cycles (96^{o}C for 30 sec, 50^{o}C for 15 sec, 60^{o}C for 2:00 min). Samples were purified by ethanol precipitation (see section 2.2.3) and then submitted to MBSU for sequencing.

2.3.8 Quantitative PCR (qPCR)

Extracted DNA from the methane biofilter was further purified by passage through a Sephadex G200 column to remove PCR inhibitors (see section 2.2.2). qPCR standards for the quantification of 16S rRNA gene and *pmoA* were prepared by amplifying 16S rRNA gene and *pmoA* from the genomic DNA of a MOB. The 27F-1492R primers (table 2.2) were used for the preparation of the 16S standards while the A189F and mb661 primers (table 2.2) were used for *pmoA* (see section 2.3.2 and

section 2.3.4). The PCR product was purified using the QIAquick PCR cleanup kit (see section 2.2.4) and then quantified using Nanodrop and Qubit (see section 2.8). Based on the average molecular weight of the amplicon and the DNA concentration, it was possible to calculate the copy number in the standards for qPCR.

From the cleaned up and quantified DNA a 10^8 gene copy/µl dilution was prepared and then serially diluted to 10^1 copies/µl. For the 16S rRNA analysis, standards from 10^3 - 10^8 copies/µl were used to standardize the quantification. For the *pmoA* analysis, standards from 10^1 - 10^6 were used for the quantification. Samples to be tested were run in triplicate with several dilutions. Dilutions from 10^{-3} to 10^{-5} were quantified for the 16S rRNA analysis and dilutions from 10^{-1} to 10^{-3} were quantified for the *pmoA* analysis.

Each 25 µl reaction contained 12.5 µl of 2X qPCR master mix (MBSU house mix), 0.2 µM of forward and reverse primer, 518R and 341F for 16S and mb661 and A189F for *pmoA*, 1 µl of template, and nuclease-free water. The samples were run on a StepOne Plus (Applied Biosystems) qPCR system with an initial temperature of 95^{o}C for 3 minutes and then for 40 cycles of amplification (95^{o}C for 30 sec, 60^{o}C for 0:30 min, and 72^{o}C for 30 sec). At 72^{o}C the fluorescent signal from each sample was recorded. The PCR cycle was followed by a melt curve analysis for 1 hour where temperatures were increased incrementally (0.5^{o}C/ measurement) from 65^{o}C to 95^{o}C. Efficiencies for analysis of *pmoA* was between 95.7% - 110.6% and was between 96.7% - 105.3% for 16S rRNA analysis.

Table 2.2 Table of primers

Primers utilized in this study, the target, application, and expected product size of each set.

Primer Pair Names	Target	Purpose					Primer Sequence (5'-3')	Expected Product Size (bp)	Reference
		RFLP	T-RFLP	DGGE	Seque-ncing	qPCR			
27F 1492R	Bacterial 16S	x					AGA GTT TGA TCM TGG CTC AG TAC GGY TAC CTT GTT ACG ACT T	1,465	Hongoh et al., 2003 Lane, 1991
27F^{FAM} 907R	Bacterial 16S		x				*AGA GTT TGA TCC TGG CTC AG CCG TCA ATT CMT TTG AGT TT	880	Hongoh et al., 2003 Muyzer et al. 1995
A189F mb661$^{(TET)}$	*pmoA*	x	x		x	x	GGN GAC TGG GAC TTC TGG **CCG GIG CAA CGT CIT TAC	510	Jugnia et al. 2009
M13F M13R	pCR2.1 MCS				x		GTA AAA CGA CGG CCA G CAG GAA ACA GCT ATG AC	200 + Insert	Life Technologies
341F 518R	Bacterial 16S			x		x	***CCT ACG GGA GGC AGC AG ATT ACC GCG GCT GCT GG	177	Juck et al., 2000 Muyzer et al. 1993

*TET: 5-tetrachlorofluorescein

**FAM: 6-carboxyfluorescein

***GC clamp: CGC CCG CCG CGC GCG GCG GGC GGG GCG GGG GCA CGG GGG GGG

2.4 DNA Electrophoresis

2.4.1 Agarose gel electrophoresis

To check the quality of extracted DNA or PCR amplicon and for contamination in PCR reactions a 1% agarose gel buffered with TAE (40 mM tris-acetate,1 mM EDTA) was used. For the large and small gel box, 5 µl of sample was mixed with 1 µl 6X loading dye (10 mM tris-HCl [pH 7.6], 0.03% bromophenol blue, 0.03% xylene cyanol FF, 60% glycerol, and 60 mM EDTA) and loaded into the well. Small gels were run for 20 minutes at 150 V while large gels were run for 40 minutes at the same voltage. For analyzing RFLP fingerprints, 10 µl of digest was mixed with 2 µl of loading dye and was loaded into the wells of a large gel buffered with TAE. The gel was run at 80 V for 90 min.

After the gels were run they were placed in an ethidium bromide staining bath (0.6 µg/ml) for 20 min to stain the DNA. Gels were then placed in bath of distilled water and destained briefly before imaging. All gels were imaged on the AlphaImager HP (Cell Biosciences) gel documentation machine.

2.4.2 Denaturing gradient gel electrophoresis (DGGE)

16S rRNA genes amplified from the Goldbar DNA samples, with a GC clamp attached (see section 2.3.1), were run on DGGE. The DGGE system used for this experiment was the DCode Universal Mutation Detection System (Bio-Rad). Prior to gel preparation, 16 cm inner and outer glass plates were washed on the inner surface (the side in contact with the gel) with 95% ethanol and scrubbed with paper towels.

After the plates were set up, 12 ml of polyacrylamide denaturing gel solution was prepared. Both the high and low concentration denaturing gel consisted of 8% polyacrylamide, 1X TAE, and water; and the polymerization was catalyzed with 100 µl of a 10% APS solution and 10 µl TEMED. For the high concentration gel, 7.20 ml of 100% denaturing solution (40% v/v formamide and 42% w/v urea) was added to the base mixture while the low concentration solution contained 4.80 ml of 100% denaturing solution. After the gradient was poured, the denaturing gels were allowed to polymerize for 1 hour. Four millilitres of stacking gel (6% polyacrylamide, 1x TAE, 10 µl of 10% APS, 5 µl of TEMED, and water) were added on top of the denaturing gel and the comb was placed in. After 5 minutes, the comb was removed and the wells were washed out with a syringe containing the 1X TAE buffer to remove residual un-polymerized stacking gel.

Gels were locked into the core and then placed the electrophoresis tank containing 1X TAE. The gels were heated to 60^{o}C and then the DNA samples (between 100 and 200 ng), previously purified using PCR purification kit and quantified (see section 2.2.4) and mixed with 2x loading dye, were loaded into the wells. Two microlitres of 100 base pair DNA ladder (Fermentas) were loaded onto the gel as a marker. The gel was run initially at 200 V for 15 minutes to drive the DNA into the denaturing gel. The gel was then run at 70 V for 8 hours at 60^{o}C to allow the bands to separate.

After running, the plates were opened and the stacking gel was removed. The gel was placed into a Sybr Gold, 1X TAE stain bath (1x SYBR Gold, Life Technologies) for 45 minutes. The gel was then moved to a 1X TAE destain bath for another 45 min. The

gel was imaged on the gel documenter. After imaging the gel photo was analyzed using Gel Compar II (Bionumerics). See section 2.10 for further information.

2.5 Restriction Fragment Length Polymorphism

2.5.1 Cloning of PCR amplicon into pCR 2.1 TOPO TA Vector

Fresh PCR product for the 16S rRNA gene RFLP and gel purified gene product for the *pmoA* RFLP was used for cloning into a pCR® 2.1 Topo TA (Life Technologies) vector (as per manufacturer's instructions). A solution of 4 µl of PCR product, 1 µl of a salt solution (1.2 M NaCl, 0.06 M $MgCl_2$), and 1 µl of vector was prepared for the insertion of the amplicon into the vector. After mixing, the solution was allowed to incubate at room temperature. Following the incubation, the transformation of One Shot® *E. coli* Top10 chemically competent cells (Life Technologies) could proceed (see next section 2.5.2).

2.5.2 Transformation of PCR 2.1 Topo vector into chemically competent Top10 *E. coli*

After the vector was prepared with the desired insert (see previous section 2.5.1) the vector could then be transformed into Oneshot Top10 *E. coli* chemically competent cells. One tube of competent cells was thawed on ice and then 5 µl of the cloning reaction was added to the thawed cell suspension. After gently mixing, the cells were incubated on ice for 30 minutes and then heat shocked in a 42^{o}C water bath for 30 seconds. After heat shock the cells were immediately placed on ice for 2 more minutes. Room temperature super optimal broth with catabolite repression (SOC) was added

(250 µl) to the cell suspension and the cells were incubated at 37^{o}C for 1 hour on a shaker set to 225 rpm.

After incubation, the cells were spread onto pre-warmed LB agar plates with ampicillin (100 µg/ml) and X-Gal. In order to ensure that there would be enough well isolated colonies, plating was done in duplicate volumes of 10, 25, and 50 µl. After 12 hours of incubation the plates were removed from the incubator and the transformants were ready to be screened (see next section 2.5.3).

2.5.3 Blue- white screening of transformants and recombinants

White colonies (colonies containing the vector and insert) were picked for the clone library. At least 70 white colonies were picked for each sample for further screening by PCR. The colonies were picked using a sterile 10 µl pipet tip and transferred either directly to a grid plate (containing LB agar, 100 µg/ml ampicillin, and XGal) or to a 200 µl tube containing low TE and then to a grid plate. Colonies would then assigned an identity based on their position on the grid plate. Cells resuspended in low TE were placed at -20^{o}C for storage. Grid plates were incubated for a further 12 hours. Cell suspension or colony mass was then used as template for the PCR (see section 2.3.6) to amplify the insert using primer sets the border the multiple cloning site (and insert location) on the plasmid vector.

2.5.4 Enzymatic digest of PCR amplified insert

After the insert was amplified from the vector by PCR, and the insert size was confirmed as matching the expected size by gel electrophoresis (section 2.4.1), the amplicon was used directly for the endonuclease digestion to generate the RFLP

fingerprints. Digest reactions (20 µl) were prepared and contained 0.5 U/µl of the endonuclease *HhaI* as per Blaire et al., 2007 and Auman et al., 2000 (95, 96)(Table 2.3), 1X NEB buffer 4, BSA (0.1 µg/µl), and 10 µl of amplicon from the vector. Digests were prepared on ice and then incubated overnight at 37^{o}C. RFLP fingerprints were resolved on a 1.5% or 2% gel by agarose gel electrophoresis (see section 2.5.1).

2.5.5 RFLP Pattern Analysis and Sequencing

After categorization of the RFLP patterns, the different types of patterns were sequenced from the clones the RFLPs were generated from and then the sequences were identified searched using BLAST and the GenBank database (see section 2.10). Phylogenetic trees showing the evolutionary distance of the *pmoA* and 16S rRNA genes were constructed using Bioedit and MEGA 5.1 (see section 2.8 for more information).

2.6 Terminal-Restriction Fragment Length Polymorphism

Information regarding the PCR amplification of amplicon for T-RFLP from the Goldbar DNA template is available in section 2.3.3 and 2.3.5. After the amplification of labeled PCR product the reaction was purified with the QIAquick PCR purification kit.

2.6.1 Klenow fragment treatment

Prior to endonuclease digestion of the fluorescently labeled DNA, the PCR product was treated with Klenow fragment polymerase to prevent the generation of pseudo-T-RFs derived from single stranded DNA amplicon. Each reaction contained 40-50 µl of purified PCR product, 0.5 µl of Klenow fragment, 4 µl of buffer, and 0.5 µl of 2

mM of dNTPs. Reactions were incubated at 37^{o}C for 30 minutes and then the enzyme was inactivated by incubation at 75^{o}C for 20 minutes.

2.6.2 Enzymatic digest of amplicon to generate T-RFs

After treatment with Klenow fragment the amplicon was purified with the QIAquick PCR purification kit (see section 2.2.4) and then quantified by Nanodrop. After purification, 250 ng of DNA was digested to generate the T-RFs. The amplified 16S rRNA gene was digested with *MspI, AluI,* or *RsaI* (New England Biolabs) while *pmoA* was digested with *HhaI* or *RsaI* (table 2.3). Each reaction contained 250 ng of DNA, enzyme (1 U), 1x CutSmart buffer (NEB), and nuclease free water.

2.6.3 DNA 3730 T-RF sequencing

For T-RF sequencing, 30 ng of DNA was mixed with 8.0 µl of HiDi Formamide buffer and 0.25 µl of GeneScan 500 TAMRA internal standard (Applied Biosystems and Life Technologies). The solution was incubated at 95^{o}C for 5 minutes to denature DNA secondary structures and then cold shocked on ice. Next, the samples were loaded onto the ABI 373A automated DNA sequencer for automated electrophoretic separation on a 5% polyacrylamide gel using GeneScan mode. Electropherograms from the samples were retrieved from the sequencer and were analyzed using GeneMapper and STAMP (see section 2.9.4).

Table 2.3 Table of restriction endonucleases used in this study with recognition sequence and cutsite. All enzymes were obtained from NEB, utilized CutSmart Buffer, and had an optimal incubation temperature of 37^{o}C.

Restriction Endonuclease	Cut site (5' - 3')
MspI	C|CGG GGC|C
AluI	AG|CT TC|GA
RsaI	GT|AC CA|TG
HhaI	G|CGC CGC|G

2.7 Gas Chromatography

Methane and carbon dioxide from gas samples taken from the methane biofilter were measured by gas chromatography. The measurements were made using a GC (Shimadzu) with a thermal conductivity detector (GC-TCD), and a HayeSep Q column. Standards for analysis were prepared from a 95% CH_4 and 5% CO_2 mix for methane and a 100% CO_2 for the CO_2 standard (Praxair). Oven temperature was set to 35^{o}C and the injection/detection temperature was set to 120^{o}C.

2.8 DNA Quantification

DNA concentration was measured spectrophotometrically by Nanodrop 2000 (Thermo Scientific). A sample of 1.5 µl was loaded onto the Nanodrop for analysis. In nucleic acid quantification mode, the DNA concentration was measured by absorbance at 260 nm and the quality of the DNA was assessed by measuring rations absorbance at 260 nm, 230 nm, and 280 nm.

DNA was also measured fluorometrically using the Qubit® Fluorometer (Life Technologies). Prior to analysis the samples were diluted 10-fold to ensure that concentrations were within the limit of detection. Each time samples were analyzed the Qubit device was standardized with 0 ng/µl and 20 ng/µl DNA standard (provided by Life Technologies). Sample (1 µl) was mixed with 1 µl of Qubit fluorescent dye ("component A") and 198 µl of buffer then incubated at RT for 2 minutes, and then measured on the fluorometer within 30 minutes.

2.9 Bioinformatics Analyses

2.9.1 Sequence analysis by BLAST

Sequenced 16S rRNA and *pmoA* from the clone libraries were searched against the GenBank database using the Basic Local Alignment Search Tool (BLAST). Nucleotide sequences were uploaded onto the BLAST website and searched using nucleotide BLAST (blastn), searching in megablast mode. Alternatively, *pmoA* was translated into amino acid sequence using ExPASy or Geneious and then searched using protein BLAST (blastp).

2.9.2 Phylogenetic analysis of *pmoA* and 16S rRNA gene sequences

Amino acid phylogenetic trees of *pmoA* were constructed by first aligning the sequences in BioEdit using the ClustalW multiple alignment. After alignment, the sequences were degapped and then imported into MEGA 5.2. In MEGA a neighbour-joining tree was then constructed (10,000 bootstraps). Similarly, 16S rRNA gene sequences were aligned in BioEdit and then imported in MEGA and analyzed using the same parameters.

2.9.3 DGGE analysis by Gel Compar II

Images of the DGGE gels were imported into the Gel Compar II software (Applied Maths) for analysis. Lanes were first divided into strips and realigned based on the positions of the DNA ladder loaded onto the gel. DNA bands were identified using the auto search function and assigned bands were manually checked and corrected as

needed. Samples were analyzed by constructing a phenogram using the DICE cluster analysis with a bootstrap of 1000 replicates.

2.9.4 Statistical Analysis of Metagenomic Profiles (STAMP) of T-RFLP

T-RFs below 50 bases and above 500 bases were filtered from the final dataset. Using GeneMapper, a minimum signal (100 fluoresence units) was used to filter out background signal from the data set. After filtering, the T-RFs were manually binned according to the average size of each T-RF size from the sample run (rounded to the nearest base). The total fluorescence for each sample was summed and the relative fluorescence of each T-RF was calculated accordingly:

$$Relative\ Fluorescence\ Units\ (RFU) = \frac{Fluorescence\ Units}{Total\ Sample\ Fluorescence}$$

The RFU was imported into STAMP for analysis. A two sided t-test (equal variance) was performed on the data and a principal component analysis (PCA) plot was generated. A heat-map of the TRFs displaying the RFU of each T-RF was also generated and included a phenogram constructed using UPGMA cluster analysis.

2.10 Enrichment of MOB from the methane biofilter

NMS medium was used to enrich MOB from the methane biofilter. Unseived biofilter medium (1 g) was added to 250 ml of NMS medium and the mixture was incubated at 30^{o}C with methane until the culture appeared to be turbid. Once turbid the culture was streaked out onto a NMS agar plate and then incubated in a growth chamber at room temperature, with methane until colonies had formed. Single colonies were picked and inoculated into 4 ml of NMS media, in 12 ml serum vials, with methane,

and incubated again at 30^{o}C until turbid. To check for contaminants, 100 µl of turbid medium was plated onto nutrient agar to check for heterotrophic contamination. Cultures with heterotrophic contamination were restreaked and then inoculated into NMS medium and checked. This was repeated until no heterotrophic contamination was detected.

Table 2.4 Composition of the MOB enrichment medium, nitrate mineral salts (NMS) pH 6.9.

Solution	Chemical	1X NMS Media
NMS base media	$MgSO_4$	4.6 mM
	$CaCl_2$	1.55 mM
	FeEDTA	0.35%
	KNO_3	9.9 mM
	Na_2MoO_4	0.01%
	$CuSO_4$	0.05 mM
Trace Elements Solution	$FeSO_4$	0.02 mM
	$ZnSO_4$	0.01 mM
	$MnCl_2$	0.001 mM
	$CoCl_2$	0.002 mM
	$NiCl_2$	0.0004 mM
	H_3BO_3	0.002 mM
	Na_2EDTA	0.008 mM
Phosphate buffer	KH_2PO_4	2 mM
	Na_2HPO_4	2 mM

3.0 Results

3.1 Measurements of methane, carbon dioxide and gas flow from the methane biofilter

This project was initially intended to monitor the methane biofilter to ensure that is was eliminating methane produced by the bioreactor effectively. Methane input into the biofilter from the bioreactor began several weeks prior to the start of the sampling for this study. Monitoring of flux gas emitted from the biofilter indicated transient methane emissions during the month of May 2011(data not shown). Post May 27, 2011 no further methane emissions from the biofilter were detected, indicating complete consumption.

There were three phases of methane input into the methane biofilter from the digesters during the sampling period. The first phase was from May 6th to June 28th 2011 during which both the test and control digesters were producing methane. On June 7th, 2011 the test digester crashed and the gas flow rate dropped substantially (control digester continued to operate till June 22nd, 2011) (Figures 3.1 and 3.2). Following the first phase the digesters were shut down and methane input into the biofilter ceased starting the second phase. The methane input resumed in September, 2011 beginning the third phase. It was not possible to sample during the beginning of the third phase due to high levels hydrogen sulphide production from the digesters. Monitoring of the third phase began on October 6th and continued until January 2012 at which point the project ended.

Methane output during phase 1 averaged 43.5% (+/- 6.3%) v/v of feed line gas. The flow rate over this time, but prior to the crash of the test digester was 78.5 L/hour (+/- 14 L/hr) and after the crash was 27.5 L/hr (+/- 0.7 L/hr). The flow rate of the control digester was 26.3 L/hr (+/- 6.6 L/hr) during the first phase. During phase 3 the methane output from the digester comprised an average of 57.0% v/v (+/- 5.7%) of feed line gas (Figure 3.1). The flow rate from the test digester was an average of 68.2 l/hr (+/- 10.9 L/hr) and was on average 53.3 L/hr (+/- 13.7 L/hr) for the control digester during this time (3.2).

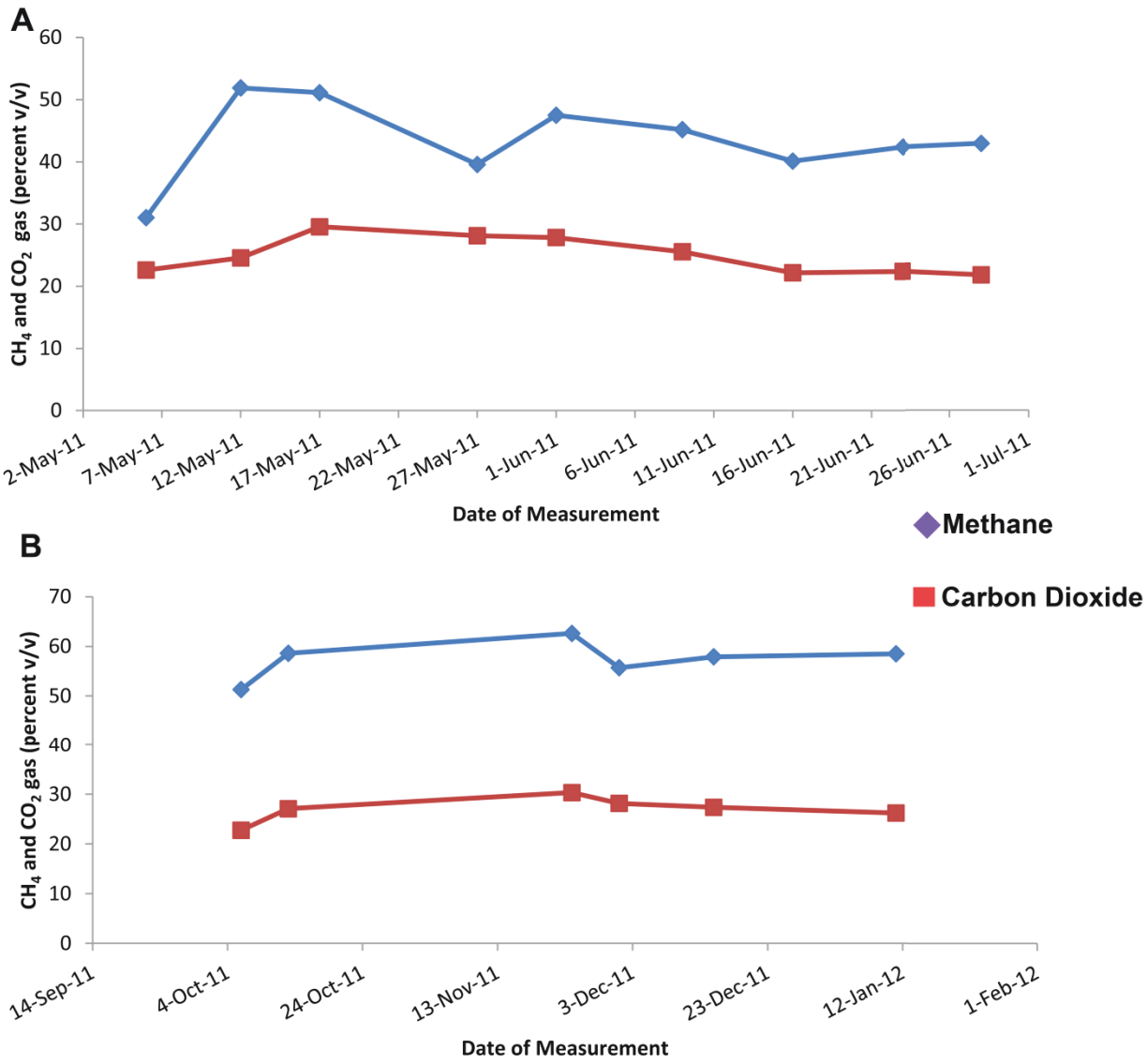

Figure 3.1 Measurements of methane and carbon dioxide input into the methane biofilter

Percent (v/v) methane (diamonds) and carbon dioxide (squares) of the methane biofilter feed line gas sampled from May 12 to June 28, 2011, phase 1(part A), and from October 4, 2011 to January 12, 2012, phase 3 (part B).

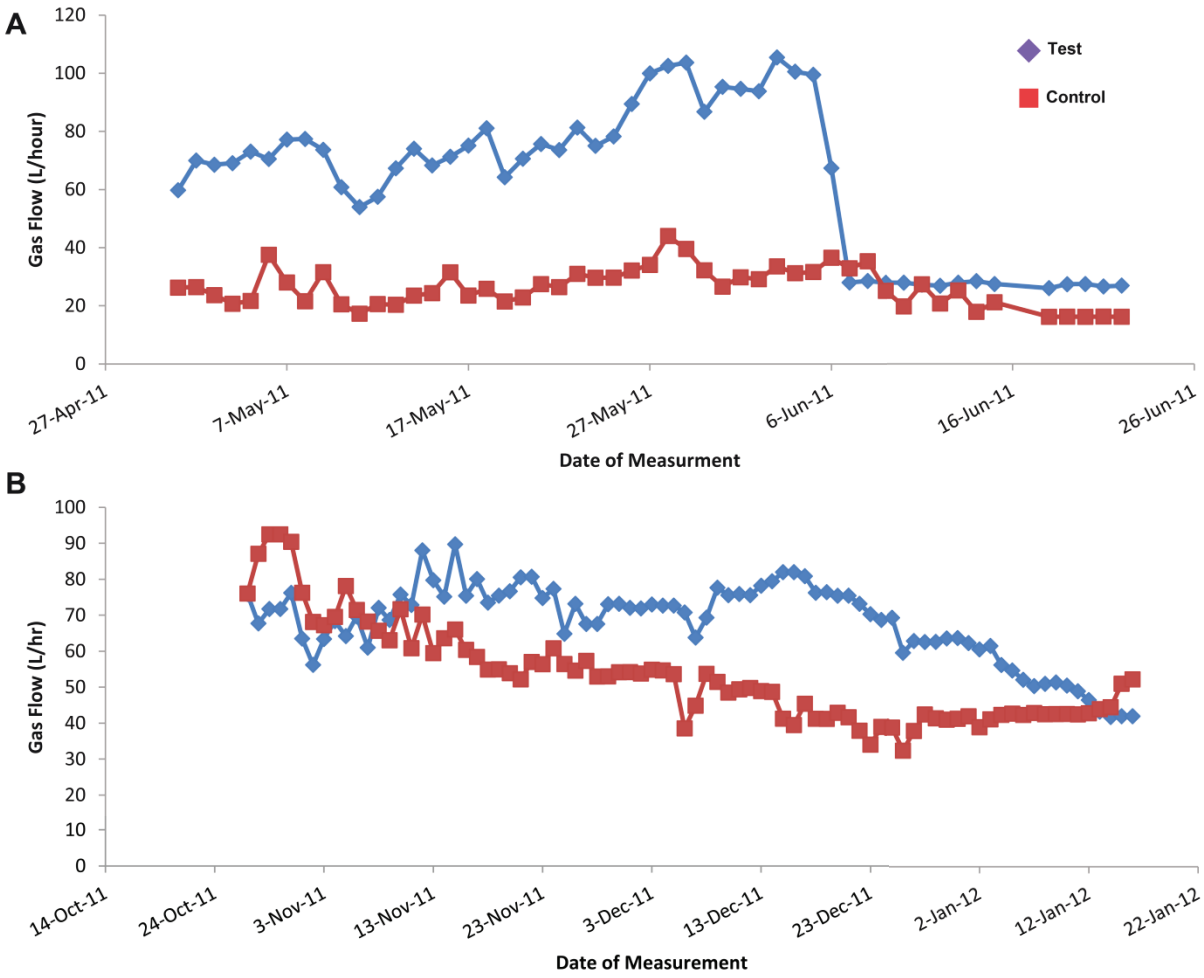

Figure 3.2 Gas flow measurements of gas produced from anaerobic digesters
Gas flow measurements (L/hour) from the test digester (diamonds) and the control digester (squares). Flow rates from the initial methane input, phase 1, are shown in part A while flow rates from the restored methane input, phase 3, are shown in part B.

3.2 Temporal study of the methane biofilter bacterial assemblage

3.2.1 Biological observations of the methane biofilter

The microbial community from across the biofilter was sampled on a regular basis to assess if the bacterial population composition varied temporally. Regular sampling occurred from May 12th, 2011 to December 1st, 2011 after which the top 10-20 cm of the biofilter compost had frozen. During the summer months a substantial number of plants grew on the biofilter. There was some variation along the length of the biofilter that was observable during sampling. Any vegetation that grew on the biofilter tended to be in the middle section of pile avoiding, in particular, the south edge of the biofilter. In addition, the center area of the pile remained unfrozen longer during the colder months than the north or south edge.

3.2.2 Denaturing gradient gel electrophoresis (DGGE) analysis of the bacterial assemblage

In order to reduce the number of clone libraries that would have to be constructed for restriction fragment length polymorphism (RFLP) analysis of the *pmoA* gene an initial survey of the bacterial community of the methane biofilter by DGGE was conducted. 16S rRNA gene DGGE analysis of the bacterial assemblage over the lifespan of the biofilter indicated the presence of three separate groups of sampling dates based on bacterial community similarity (using the UPGMA clustering method). The first group included samples from dates from May 12, 2011 to June 28, 2011. The second major group of dates in the DGGE comprised two sub-groups encompassing all the other sampling dates. The first sub-group corresponds to the second (no methane

input) phase and includes samples from July 8th to August 30th. The third group of dates includes samples from September 22nd to December 1st and corresponds to the third phase where methane input was restored into the biofilter (Figure 3.3).

Regardless of sampling date, the bacterial community was 65% similar. Thus samples within the phase 1 cluster were 35% different from the second major grouping observed. Samples from phase 2 and phase 3 were 22% similar while samples within phase 2 and phase 3 were both 80% similar.

3.2.3 Terminal-restriction fragment length polymorphism (T-RFLP) analysis of the bacterial assemblage

To confirm the observation of the three different bacterial communities observed in the DGGE analysis of the bacterial was analyzed again using a different community fingerprinting methodology known as terminal-restriction fragment length polymorphism (T-RFLP). In the PCA of the bacterial community, three distinct groups of sampling dates are observable corresponding to the initial methane input phase 1, phase 2 with no methane, and the restored methane phase 3. The PCA revealed that while the no methane and restored methane groups are more similar, the restored methane and initial methane also share similarities and cluster separately from the no methane group of sampling dates (Figure 3.4). Though the March sample was an outlier from the other initial methane samples it was still more similar to the initial methane samples than to the no methane and restored methane input (Figure 3.4).

The grouping observed in the PCA plot was also evident when the samples were displayed as a heat map with the samples clustered using UPGMA analysis. Dates

clustered in a similar fashion to the clustering pattern observed in the DGGE analysis where there are two major clusters. The first major cluster in the T-RFLP heatmap corresponds to the initial methane input phase while the second major cluster contains two subclusters that encompass the no methane phase and restored methane times phase (figure 3.5).

Several terminal-restriction fragments (T-RFs) were more abundant or completely unique to certain clusters. Of note, the fragment sizes 155, 191, 87, 166, and 279 bps were far more abundant during the initial methane input period. Fragments at 277 and 83 were present in all initial methane samples, but absent in the no methane and restored methane samples. No other cluster had fragments that were common within the sample cluster, but unique from other clusters. Fragments 148, 395, 158, 138, 164, and 436 bp were common to all samples, with the 148 bp fragment being of a particularly high abundance. Only two fragment sizes (61 and 71 bp) were unique to the second major cluster (figure 3.5).

In silico digestion of the MOB *Methylobacter* sp. BB5.1 produces a fragment of about 446 bp, which was observable in some of the samples in the T-RFLP analysis, but it is impossible to conclude for certain if this fragment really corresponds to the *Methylobacter* genus. Fragment sizes corresponding to the other dominant MOB genus in the biofilter, *Methylomicrobium*, were not detected by the T-RFLP analysis.

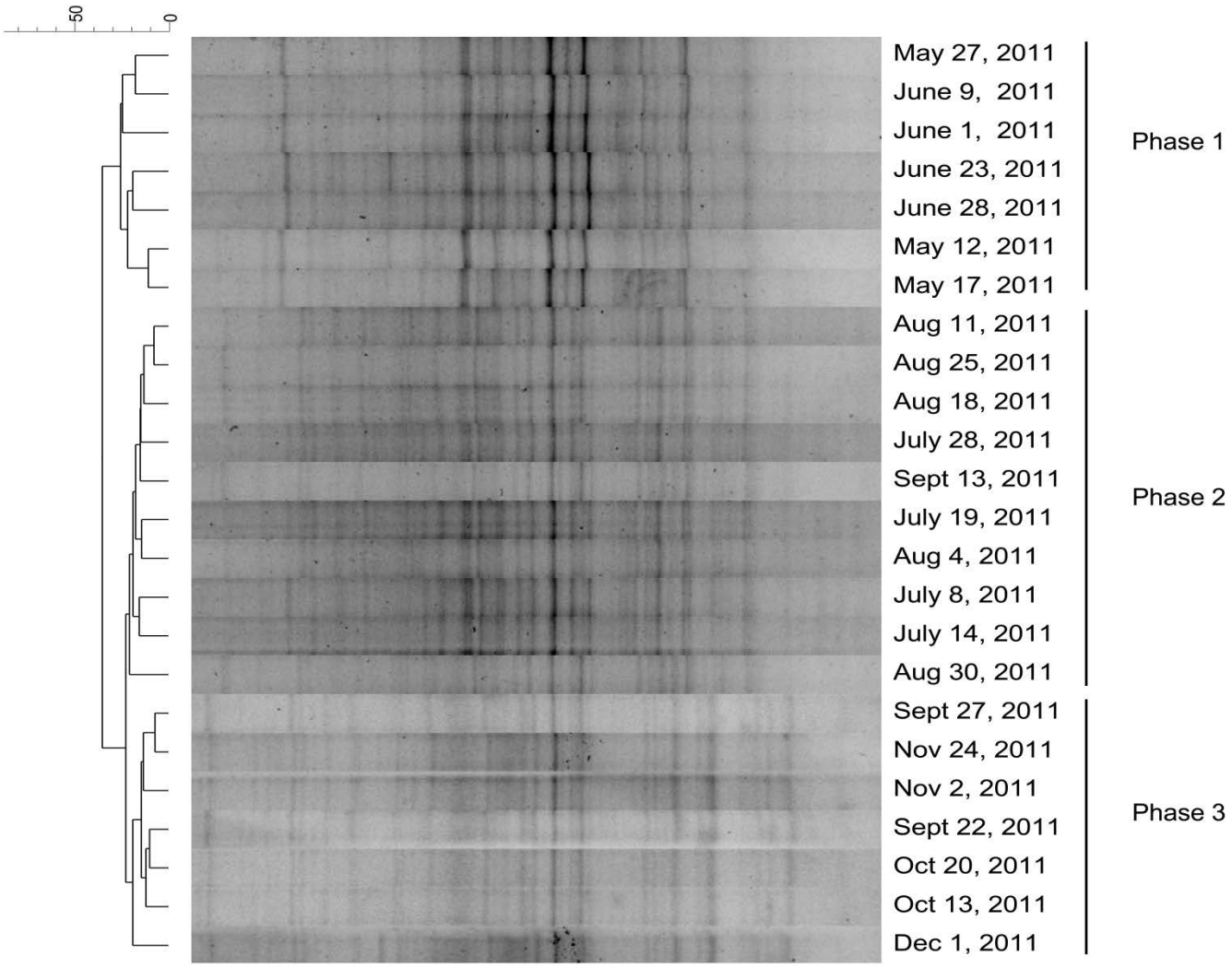

Figure 3.3 DGGE fingerprinting of the bacterial assemblage over time
16S rRNA DGGE targeting the bacterial assemblage in the methane biofilter. Sequences were amplified by PCR using the primer set 518R and 341F (with a 5' GC-clamp). Samples were run on a 8% polyarcylamide gel with a 40%-60% denaturing gradient at 70 V for 8 hours. Cluster analysis was performed using DICE with 1% position tolerance. Phase 1 constitutes the initial methane input during May and June 2011. Phase 2constitutes no methane input during July, August and early September. Phase 3 constitutes the restored methane input from late September to early January 2012.

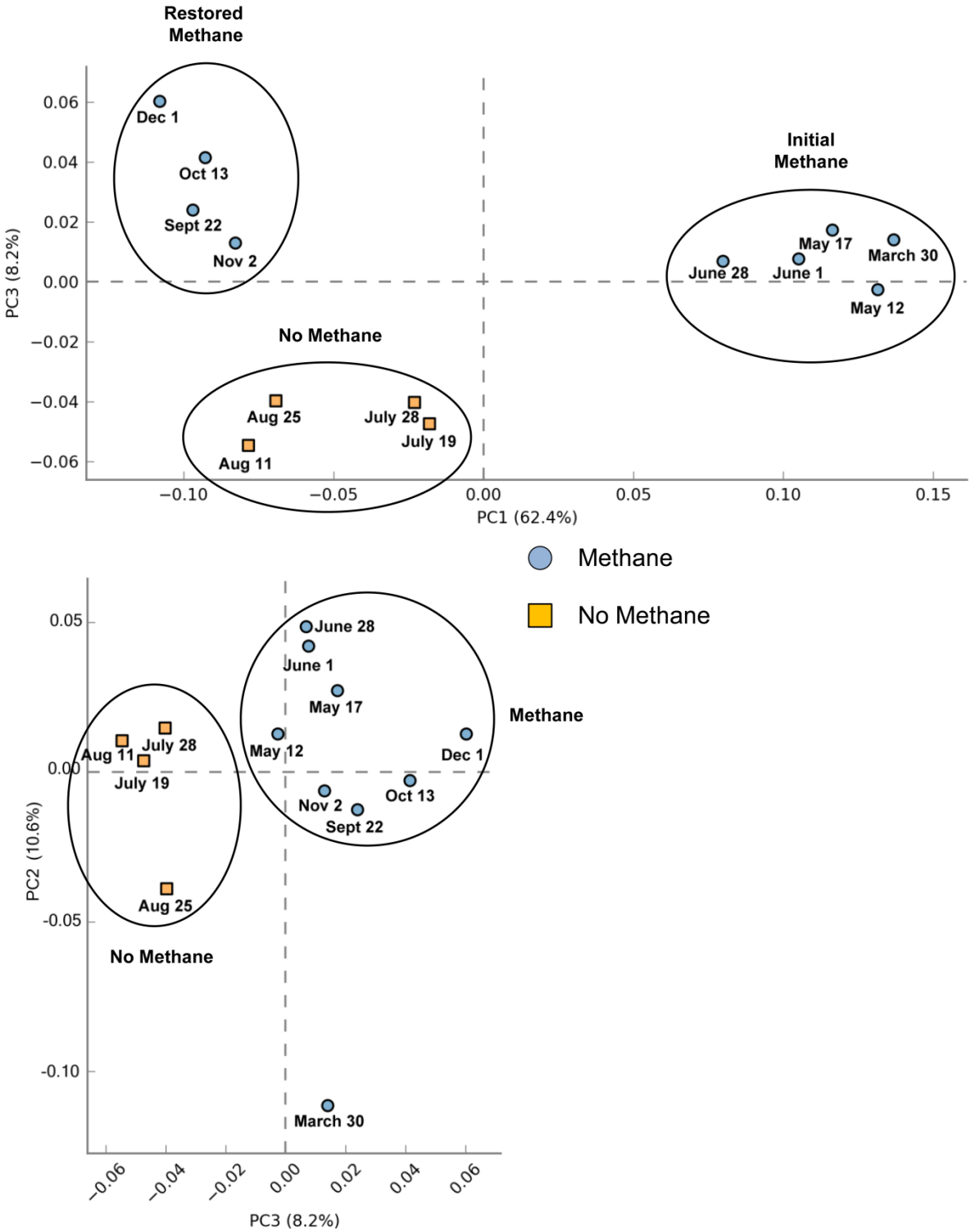

Figure 3.4 PCA analysis of the bacterial assemblage by T-RFLP fingerprinting of 16S rRNA genes

Principal component analysis (PCA) plots of the T-RFLP from several of the methane biofilter soil samples. T-RFs were generated by amplifying bacterial 16S with FAM-labeled 27F and 907R followed by digestion with *MspI* endonuclease. PCA was calculated using an ANOVA ($p < 0.05$).

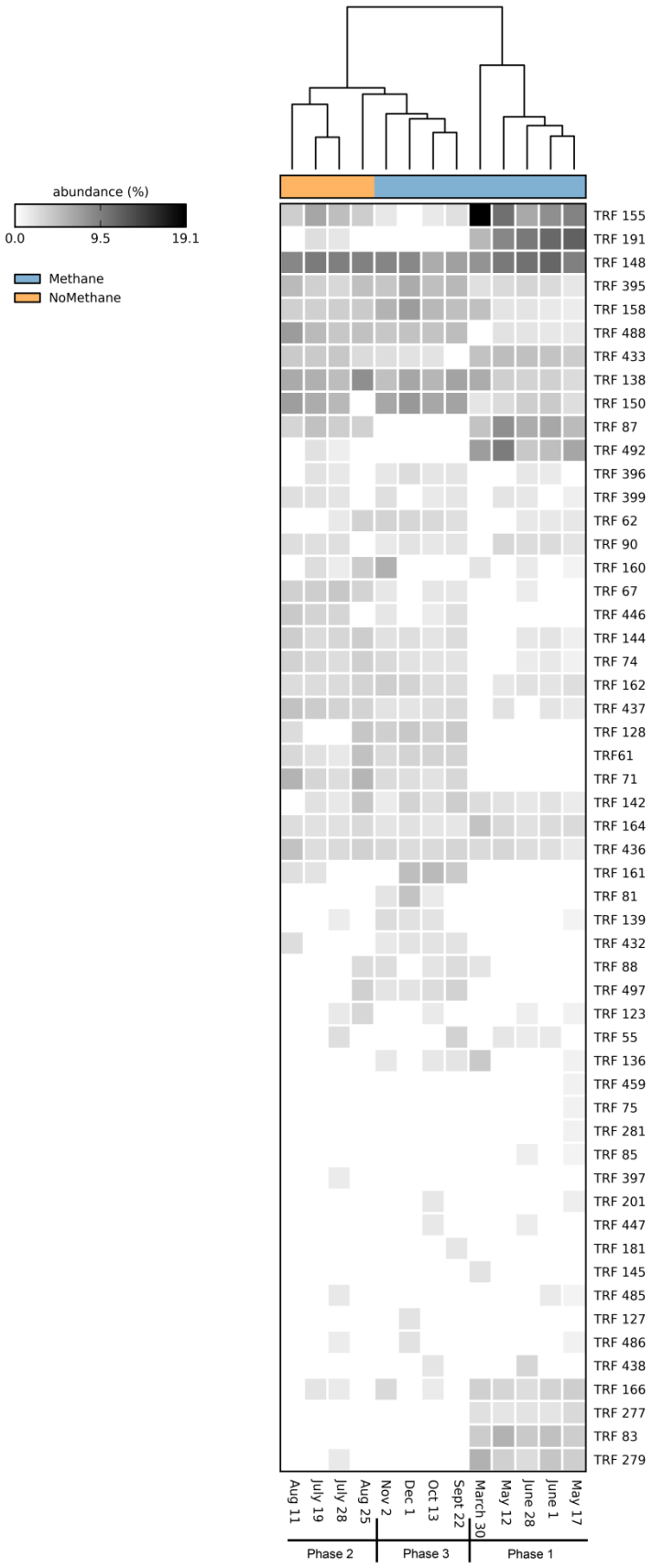

Figure 3.5 Heatmap analysis of the bacterial assemblage by T-RFLP fingerprinting of 16S rDNA

T-RF heat map analysis of several methane biofilter soil samples. T-RFs were generated by amplifying bacterial 16S rRNA genes with FAM-labeled 27F and 907R followed by digestion with *MspI* endonuclease. The relative abundance of each T-RF (measured by RFU) is represented by the shade of each square (light shade: less abundant, darker shade: more abundant). The sample phenogram was constructed by using UPGMA cluster analysis.

3.3 Methane oxidizing bacterial assemblage in the methane biofilter

3.3.1 Phylogenetic analysis of *pmoA* clone library sequences

Based on the information provided by the analysis of the bacterial assemblage using DGGE and T-RFLP, two sampling dates per phase were chosen to do a more in depth study of the MOB assemblage within the biofilter. Although a total of eight restriction fragment length (RFL) patterns were identified, the phylogenetic analysis of the sequenced clones indicated that several types originated from the same OTU (figure 3.6). These RFLPs were collapsed together to represent a single OTU. Based on this reasoning, eight RFLP types were condensed to four RFLP types (OTUs) representing four different genera. These genera include *Methylobacter*, *Methylomicrobium*, and *Methylocaldum* from the phylum *Gammaproteobacteria* and *Methylocystis* from the phylum *Alphaproteobacteria* (Figure 3.6).

The majority of the *Methylobacter* related clones grouped most closely with the *Methylobacter* sp. BB5.1. One *Methylobacter* clone (clone21) was distinct from other OTUs and clustered with the species *Methylobacter* sp. CMS7 and with a clone from a landfill biocover soil. The *Methylomicrobium* related clones clustered with the *pmoA* gene from *Methylomicrobium album.* Within this cluster a clone from a landfill biocover study was also present as well as a clone from the MOB enrichment experiment. Two other less abundant OTUs were also present. Clone17 was most closely related to *pmoA* from the genus *Methylocaldum,* specifically the species *M. gracile*. Clone19 clustered with *pmoA* from the *Methylocystis* genus and was closely related to the *pmoA* gene from *M. rosea* SV97 (Figure 3.6).

3.3.2 Temporal dynamics of the MOB assemblage in the methane biofilter

Throughout the lifespan of the biofilter the MOB assemblage was dominated by two *Gammaproteobacteria* genera, *Methylomicrobium* and *Methylobacter*. The two other genera detected were *Methylocaldum* and *Methylocystis* which appeared sporadically throughout the lifespan of the biofilter (Table 3.1).

Early on in the initial methane input phase *Methylomicrobium* and *Methylobacter* comprised an equal portion of the MOB assemblage. Midway through the phase 1 of methane input the *Methylomicrobium* species became more dominant comprising more than two thirds of the MOB assemblage. In the no methane input phase 2, *Methylomicrobium* was initially dominant, but became less dominant in the latter portion of this phase where the assemblage became dominated by *Methylobacter*. In the final, restored methane, phase *Methylomicrobium* and *Methylobacter* comprised about equal portions of the MOB assemblage. *Methylobacter* was dominant by the end of the third and final phase (Table 3.1).

The less dominant OTUs, *Methylocaldum* and *Methylocystis*, were most prevalent early in the second phase (no methane input). *Methylocaldum* was only present within the first and second phases whereas *Methylocystis* was only detected in the second and third phases. These two genera never comprised more than 5% of the total MOB assemblage (Table 3.1).

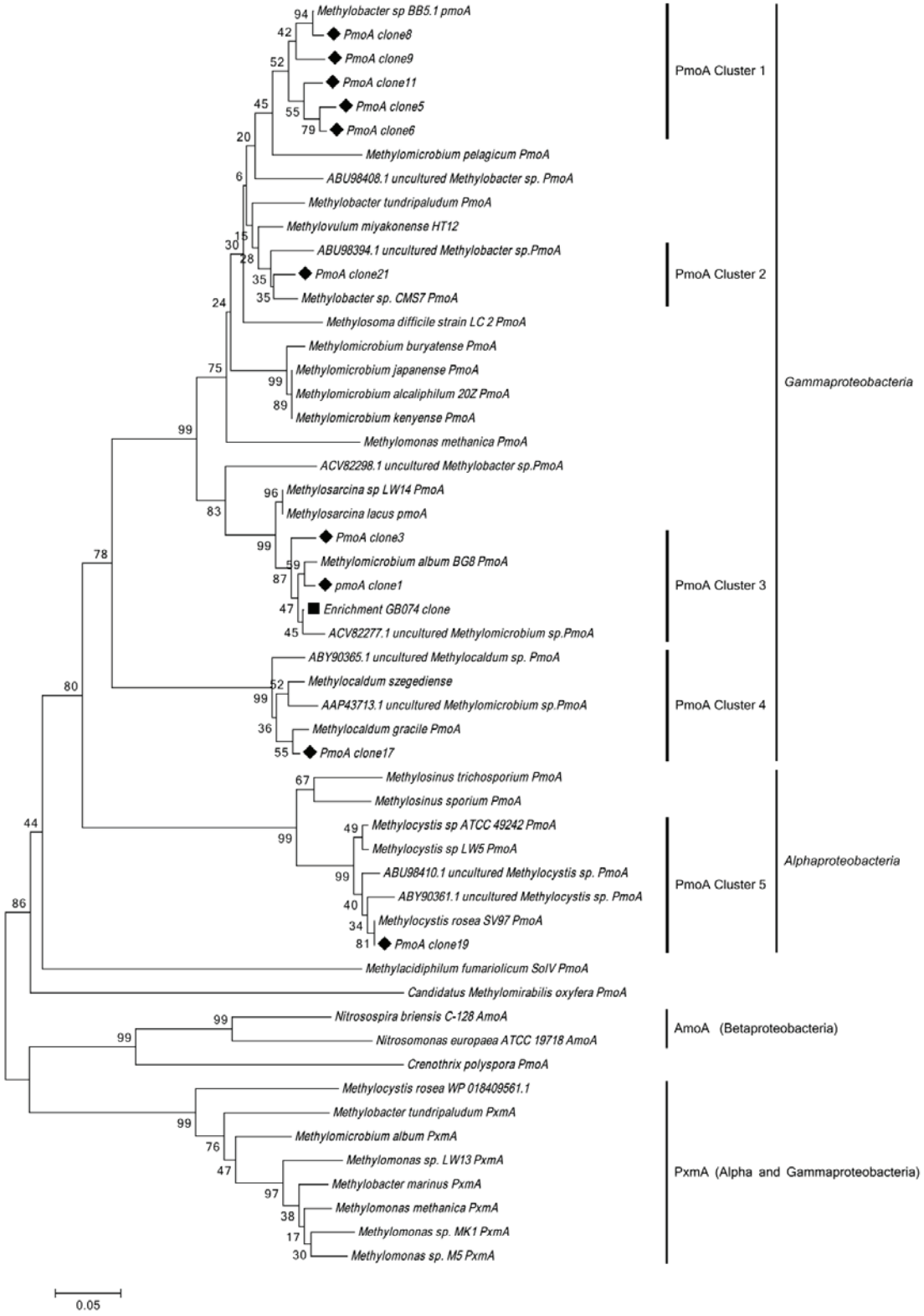

Figure 3.6 Phylogenetic analysis of translated *pmoA* clones from the methane biofilter and MOB enrichment

PmoA, amino-acid, neighbour-joining tree (10,000 bootstraps) constructed from 140 residues (MEGA 5.2) and aligned in BioEdit using the ClustalW multiple alignment tool. Bootstrap values are shown at the tree junctions and **methane biofilter clones are indicated with a diamond. The enrichment clone sequence is indicated with a square**. *pmoA* clone sequences were translated using the Geneious translation tool.

Table 3.1 Temporal variation of the MOB assemblage by RFLP
RFLPs were generated from cloned *pmoA* amplicon (A189F-mb661) digested with the restriction endonuclease *HhaI.* RFLP were grouped according to the phylogenetic analysis of the cloned genes to assign an associated genus.

Genera	methane		no methane		methane	
	Percent Representation in Clone Library					
	May 17	**June 1**	**July 19**	**Aug 25**	**Sept 22**	**Dec 1**
Methylomicrobium	49%	67%	59%	43%	55%	38%
Methylobacter	49%	33%	37%	55%	45%	61%
Methylocaldum	2%	0	4%	2%	0	0
Methylocystis	0	0	2%	0	0	1%
Total clones	47	61	54	60	62	64

3.4 Enrichment of MOB native to the methane biofilter

As a point of interest, an attempt was made to cultivate MOB from the methane biofilter. The enrichment of MOB from the methane biofilter yielded a single, enriched *Methylomicrobium*-related species of MOB based on 16S rRNA gene sequencing (Figure 3.6). Sequencing of the *pmoA* gene demonstrated that the enriched MOB was most similar to *Methylomicrobium* and the sequence clustered with *pmoA* clones from the methane biofilter. Both the 16S and the *pmoA* sequences indicate that this *Methylomicrobium* was most closely related to *M. album* and *M. agile* (Figure 3.7).

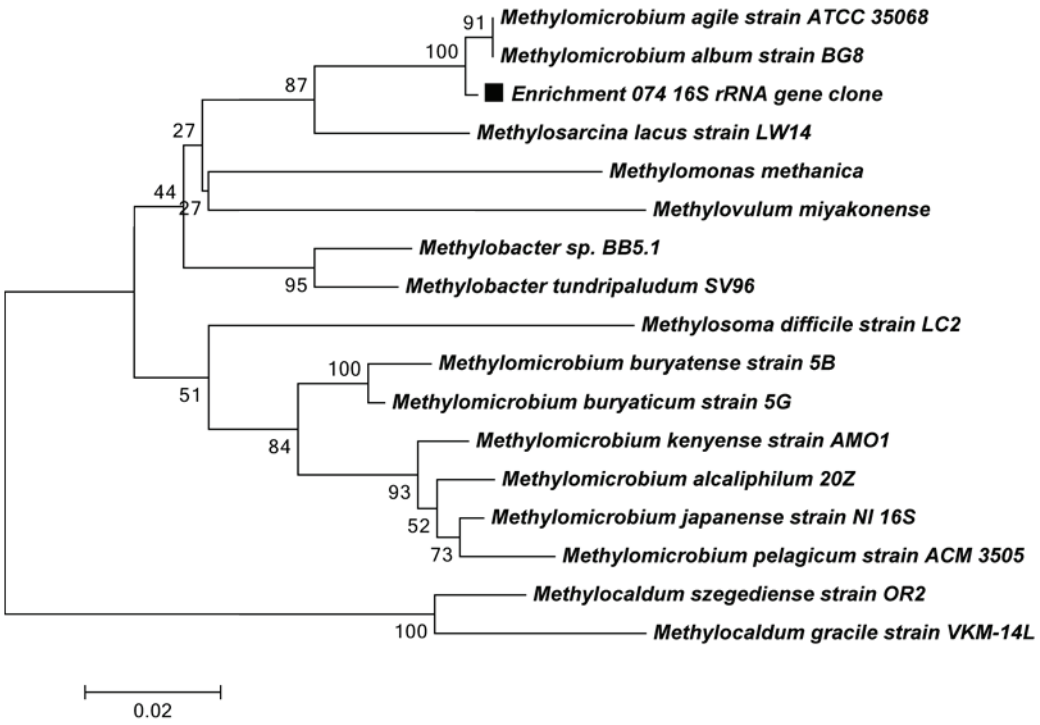

Figure 3.7 Phylogenetic analysis of the 16S rRNA gene MOB clone from the methane biofilter MOB enrichment

16S rRNA gene, nucleic-acid, neighbour-joining tree (10,000 bootstraps) constructed from 359 bp (MEGA 5.2) and aligned in BioEdit using the ClustalW multiple alignment tool. Bootstrap values are shown at the tree junctions and the enrichment clone is indicated with a square.

3.5 Quantification of the total bacterial and MOB community in the methane biofilter

To assess how the numbers of MOB and the number in the total bacterial community in the methane biofilter changed in response to the methane input quantative PCR (qPCR) was employed. The number of MOB present in the methane biofilter was measured by quantifying the MOB marker gene, known as *pmoA*. The total bacterial community was measured by quantifying the bacterial 16S rRNA genes.

The total bacterial and MOB assemblage was quantified by qPCR analysis of the bacterial 16S rRNA gene and *pmoA* (Figure 3.8). The total number of 16S rRNA genes was significantly higher during the initial methane input period ($p<0.05$). After methane input ceased, the number of bacteria decreased significantly ($p<0.05$). When methane input was restored there was no significant increase in the copy number of bacterial 16S rRNA genes ($p<0.05$). The *pmoA* copy number was significantly higher ($p<0.05$) during the initial methane input period. The copy number of *pmoA* genes then declined significantly when methane input ceased ($p<0.05$). *C*opy number of *pmoA* increased significantly again once methane input was restored to the biofilter ($p<0.05$) (Figure 3.8). Melt curve analysis showed the presence of two distinct melting temperatures in the *pmoA* qPCR. When the *pmoA* qPCR amplicon was checked on a gel only one band was present. This indicates that there are two dominant sequences of *pmoA* present within the sample.

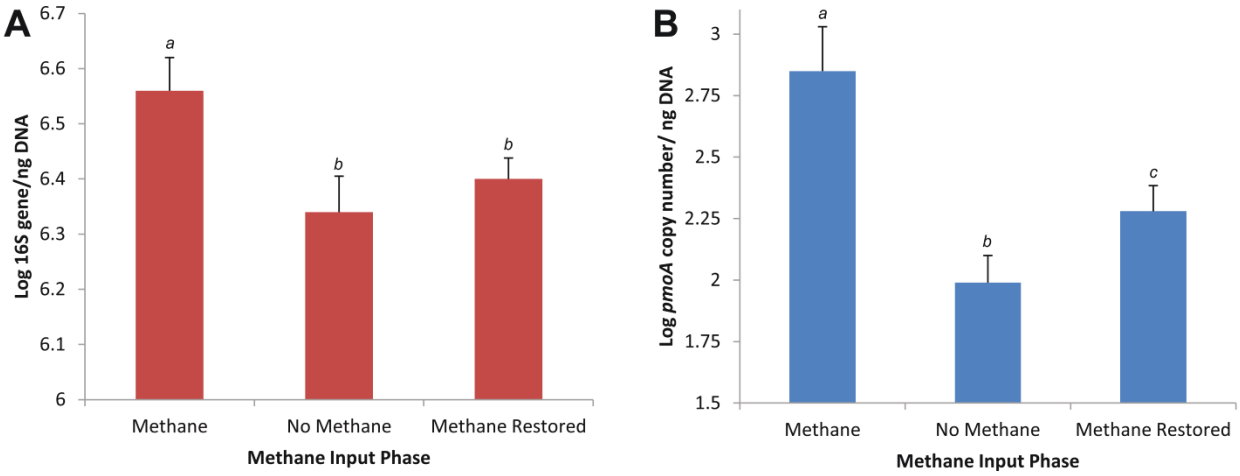

Figure 3.8 Quantification of *pmoA* and bacterial 16S rRNA genes from the methane biofilter by qPCR

Gene copy number was normalized to the ng of DNA per qPCR reaction. The mean and standard error of the gene copy number for each period (initial methane, no methane, and restored methane) was calculated (*n=4*). Each period was compared using a one-way ANOVA ($p<0.05$) to determine the significance. **A** 16S rRNA gene copy number from the biofilter: *a* significantly different from *b*. **B** *pmoA* copy number from the biofilter: *a* significantly different from *b* and *c*, *b* is significantly different from *a* and *c*, *c* is significantly different from *a* and *b.*

4.0 Discussion

4.1 The effect of methane input on the methane biofilter bacterial assemblage

DGGE analysis of the bacterial assemblage revealed three distinct clusters that corresponded to the phases of methane input into the biofilter. The May-June cluster corresponded to the initial methane input phase, the July-August cluster corresponded with the no methane input phase, while the September-December cluster corresponded to the final, restored methane input phase (Figure 3.3). The T-RFLP analysis of bacterial 16S rRNA genes supported this clustering of sample dates (Figure 3.4). Rapid changes in the bacterial community composition were observed in samples that bridge the transition from phase 1 to phase 2 and phase 2 to phase 3, in the span of less than 2 weeks. This contrasts the relatively stable bacterial community that is present during the months prior to these sudden changes in methane input. This also lends support to methane influencing the bacterial community composition. Analysis of the evenness and diversity of the community by the Shannon-Wiener index indicates that though the community changed, the evenness and richness did not change ($P<0.05$) (Table 4.1).

Very few studies have examined how the overall bacterial assemblage of a given environment is affected by methane input. One study by Wang et al. 2008, that examined the bacterial diversity of a bench-top scale, simulated landfill bio-cover demonstrated that the presence or absence of methane affected the bacterial diversity in the bio-cover (97). Another interesting component of that study was the effect of vegetation on the bacterial community. Wang et al. demonstrated that the presence of the plant species *Chenopodium album*, a weedy annual plant, also influenced the

bacterial assemblage composition. This could also have affected the bacterial assemblage composition in the current study as many plants took root in mid-June; however, the plant growth cannot account for sudden changes in the bacterial community composition that was observed from June to July of 2011.

Another possibility could be moisture levels in the methane biofilter. The biogas generators could input moisture into the biofilter, however water vapor was not detected during the GC analysis in the input gas. In addition, data provided by the Government of Canada indicated that average monthly rainfall was highest during June and July of 2011 and much lower in other months, 140 mm and 120 mm in June and July respectively and less than 20 mm in other months (Figure 4.1- B). This does not correspond to the pattern of the relatively distinct microbial communities observed.

Ambient temperature could have also have affected the bacterial community composition. However, the methane biofilter itself generated internal heat from the decay of the MBF medium. Changes in temperatures from month were relatively minor (Figure 4.1- A) and the pattern of temperature change was not obviously reflected in the bacterial community composition. Outside physical factors including temperature and precipitation seemed to have a limited effect on the bacterial community composition. Furthermore rapid changes in the bacterial community composition cannot be explained solely by external physical factors indicating that methane is likely a major driver of community composition.

A possible mechanism by which methane affects the bacterial community is due to its role as an initial carbon and energy input into an environment. In a scenario

where methane is a major component of the carbon and energy input into the environment, the MOB are the primary producers (98, 99). The members of the bacterial community at higher trophic levels are likely also affected by which primary producers are present and likely respond to any switch in the identity of the primary producer . Any major change, such as the complete loss of methane in an environment, could shift the bacterial community towards species that are better equipped to harvest the second most prominent carbon and energy input into the ecosystem.

The importance of methane as a driver of bacterial community composition is highlighted in a study Gebert et al. 2009 (27). In this study of a landfill bio-cover MOB assemblage, Gebert et al. found that despite large variations in soil physical factors (such as pH, total organic carbon, and total nitrogen) there was very little variability in the MOB community (27). A recent study of a methane biofilter by Kim et al. examined how a perlite-based methane biofilter bacterial community changed over 108 days with stable methane input (100). The bacterial community over time remained stable, little change in species richness or evenness indicating that under constant conditions, including a consistent methane input, the diversity of a bacterial community will remain stable.

Quantitative PCR data showed that the initial bacterial community in phase I was larger than succeeding communities in phases II and III (Figure 3.8). There was a significant decline in the total number of bacteria when methane input into the biofilter ceased (Figure 3.8). There was no significant increase in the number of bacteria when methane input was restored ($P < 0.05$) (Figure 3.8). This may indicate that methane was

an important substrate in the initial bacterial community and after methane input ceased the bacterial community was unable to sustain itself and declined.

Another possible explanation is that the decline in the numbers of bacteria in the community is a reflection of the declining numbers of the MOB community (Figure 3.8). Estimating the number of MOB present in the total bacterial community seems to indicate that the percentage of MOB in the total bacterial community does not change from phase to phase. This could suggest then that the decline in the bacterial community numbers (Figure 3.8) from phase 1 to phase 2 may be due in part to the decline of the MOB community.

Table 4.1 Shannon-Wiener diversity index analysis of bacterial communities. Comparison of the diversity of the bacterial community, by T-RFLP, under different methane exposures, using the Shannon-Wiener diversity index. Each mean value was calculated from an n = 4. One-way ANOVA analysis concluded that there is no difference in H'-index value between bacterial communities (*P<0.05*).

methane input bacterial community (by T-RFLP)	Mean H'-index	H'-index Standard Deviation (+/-)
Initial methane	3.14	0.16
No methane	3.19	0.19
Restored methane	3.23	0.12

Table 4.2 Estimation of the average percent MOB in the total bacterial community in the MBF

The average number of MOB present in the total bacterial community was estimated by assuming the average copy number of 16S per bacterial genome was 4.2 (as per Case et al. 2006) and that the average number of *pmoA* copy numbers per MOB genome was 2 (as per Reim et al. 2012 and Semrau et al. 1995) (116–118). The percentage is calculated as the estimated number of MOB cells in the estimated bacterial community based on the qPCR data shown in Figure 3.8.

Methane Input	Average percent MOB in total bacterial community	
Initial Methane (Phase 1)	0.073	± 0.067
No Methane (phase 2)	0.010	± 0.005
Restored Methane (phase 3)	0.018	± 0.006

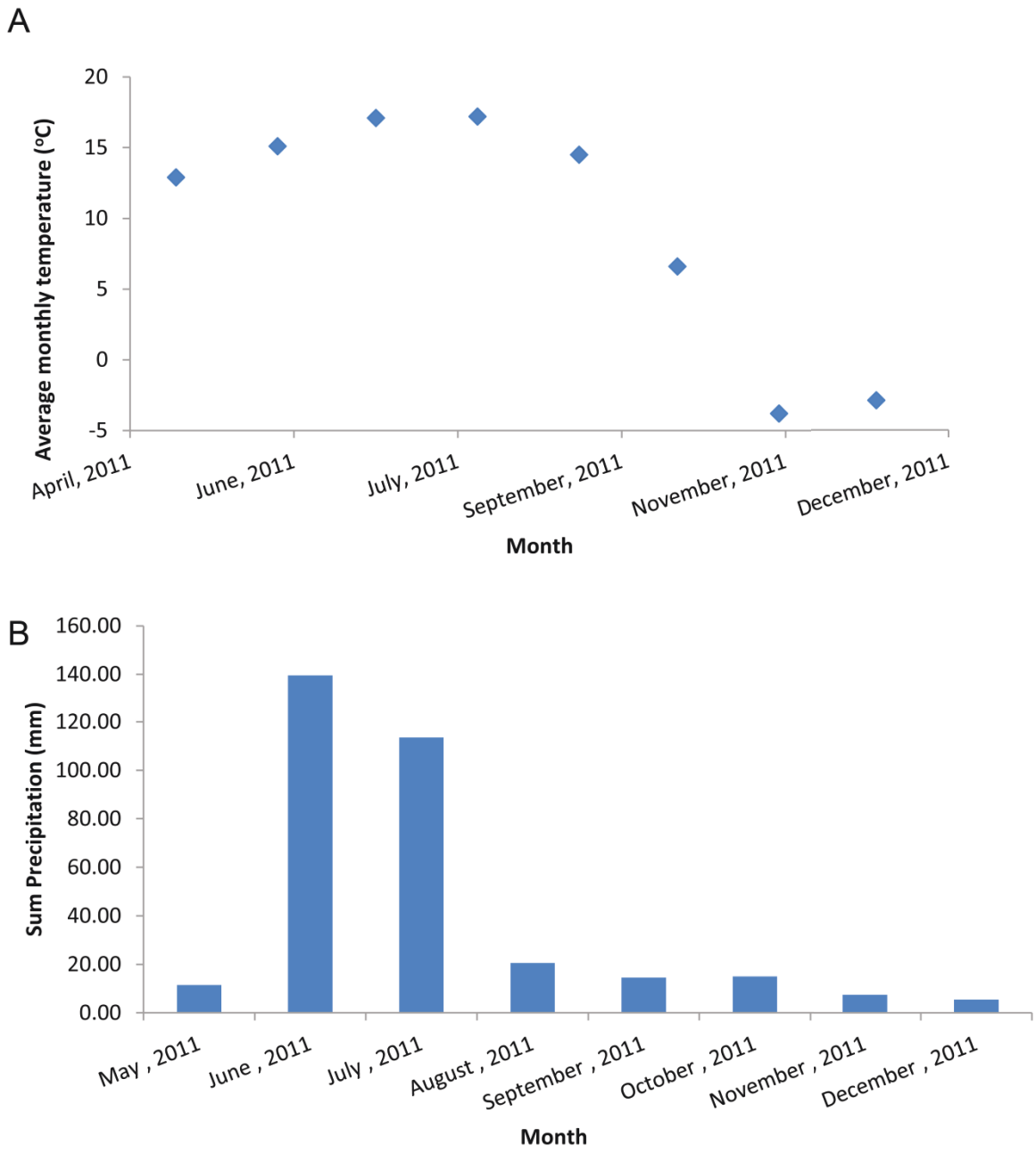

Figure 4.1 The City of Edmonton monthly temperatures and precipitation

A) Average monthly temperatures for the City of Edmonton from the city centre weather station. **B)** Summation of the monthly precipitation for the City of Edmonton from the city centre weather station. Data was collected from the Government of Canada and is available at "climate.weather.gc.ca"

4.2 The effect of methane input on the MOB assemblage

The diversity of MOB was assessed by sequencing the marker gene, *pmoA.* Clone libraries found that the MOB assemblage consisted of species from the genera *Methylobacter, Methylomicrobium, Methylocaldum,* and *Methylocystis.* Enrichment experiments yielded a *Methylomicrobium* species similar (based on *pmoA* gene sequence) to those found in the biofilter. All these genera have previously been detected in methane biofilter and landfill biocover soil studies (27, 30, 97, 100–106). Other MOB that have been detected in these systems include: *Methylococcus, Methylosinus, Methylocapsa, Methylomonas, Methylocella,*and *Methylosarcina* (27, 30, 97, 100–106). Previous studies analysed the MOB assemblage using microarray analysis, DGGE, pyrosequencing, T-RFLP, and PLFA (27, 30, 97, 100–106). Only two previous studies have provided sequence information for *pmoA* sequences from a landfill biocover and no sequences have been obtained from methane biofilters (30, 103).

Gammaproteobacteria MOB dominated the methane biofilter during the entire run of the biofilter. The most populous genus alternated between *Methylobacter* and *Methylomicrobium (*Table 3.1). Several previous studies also describe biofilter and biocovers as being dominated by *Gammaproteobacteria* MOB. The examination of a methane biofilter over 108 days by Kim et al. (89) showed dominance by *Gammaproteobacteria* from the genera *Methylocaldum* and *Methylomonas.* The dominance of these two genera only increased as the biofilter aged (100).

Jugnia *et al* suggested that *Gammaproteobacteria* MOB may be pioneer species of MOB in nascent landfill bicovers (30). According to Ménard et al., in their 2012 review of methane biofilter literature, there was no apparent environmental factor influencing the dominance of either *Gammaproteobacteria* or *Alphaproteobacteria* in any particular system (22). This conclusion is logical given the vast diversity of phenotypes exhibited by MOB within both phyla.

The less populous genera, *Methylocaldum* and *Methylocystis*, were most abundant just after methane input ceased, the beginning of phase 2. This relatively sudden appearance could have been in response to the lack of methane. However, *Methylobacter* and *Methylomicrobium* still dominated the assemblage (Table 3.1). These results do not take into account which MOB species were most active. It is conceivable that lower abundance MOB could have been more active at the points where methane input fluctuated and that the higher abundance MOB were less metabolically active.

One way to account for active and dormant MOB would be to label the active member of the MOB assemblage by stable isotope probing (SIP) with $^{13}CH_4$ in a microcosm experiment or by metatranscriptomic analysis of the biofilter soil. The SIP study by Cébron et al. on landfill biocover microcosms demonstrated that the relative abundances of active, ^{13}C labeled *pmoA* within a *pmoA* clone library was different from the relative abundance measured in the inactive ^{12}C *pmoA* clone library (101). A caveat to the SIP method is that microcosm conditions will never perfectly match field conditions and so observations from SIP may not actually reflect those in the environment.

Species evenness of MOB remained consistent between phases regardless of the presence or absence of methane. This is similar to recent observations reported by Pan et al where a disrupted MOB assemblage that was first treated by acetylene (irreversible inactivator of pMMO) and then either by kanamycin or gamma-irradiation was extremely resilient to change (106). Despite these treatments, when methane was provided, the MOB assemblage recovered and was eventually very similar in both abundance and diversity as the original, untreated, assemblage (106). That resilience appears to be supported by this study. Despite two months without any methane input, the MOB assemblage diversity remained stable.

The same stability seen in MOB community composition cannot be said of the total abundance of MOB in the methane biofilter. The population of MOB declined after the initial methane input into the system ceased (Figure 3.8). After methane input was restored to the methane biofilter the MOB population increased (Figure 3.8). The melt curve analysis indicated the presence of two distinct *pmoA* sequences in the all samples tested. This suggests that the MOB assemblage in the biofilter is dominated by two major OTUs which corresponds to the observations made in the *pmoA* clone library analysis. It is worth noting that the MOB population was able to maintain itself during the phase 2, no methane input. There are several possible mechanisms by which MOB assemblage could have sustained itself.

The MOB population could have been sustained by small amounts of methane produced within the biofilter by methanogens. Another possibility is that the MOB population became inactive to protect itself from nutrient limitations or that the MOB were able to survive on stored carbon substrates, such as poly-3-hydroxybutyrate or

exopolysaccharide (107). Such dormancy behaviour has been previously described where MOB were able to recover after 10 weeks of methane starvation, including *Methylomicrobium album,* in what the authors describe as “anaerobic dormancy” (though survival was possible aerobically as well, but survivability was reduced) (108–110). Other studies examining biofilters have found that, following starvation of the biofilter substrate (for example: toluene or hydrogen sulphide), the biofilters rapidly recovered their capacity to eliminate their respective targets (111, 112). The *Methylomicrobium* and *Methylobacter* genera are not known to be facultative MOB so it is unlikely that they continued to grow on other organic substrates (section 1.3.4).

4.3 Future Experiments

Continued analysis of the samples from the methane biofilter can enhance confidence in the final conclusions. T-RFLP should be performed on the *pmoA* gene to support the clone library data. T-RFLP has the advantage of being semi-quantitative and can provide information on which MOB species were most prominent in the assemblage. Clone libraries of the bacterial 16S rRNA gene can be constructed to give added confidence to the 16S rRNA gene T-RFLP results. The sequence information provided by the clone libraries can also give an identity to the OTUs identified in the 16S T-RFLP illuminating which members of the bacterial community were most affected by changes in methane input. Sequencing of DGGE bands could also be an option to identify major OTUs. Lastly, whole community 16S rRNA gene sequencing can provide more information on the major members the methane biofilter bacterial communities including MOB. This method is also semi-quantitative and could reinforce T-RFLP results, DGGE results, and qPCR results.

In future experiments with methane biofilter systems the collecting of physical data should be considered. Parameters such as pH, soil moisture, and especially temperature are known to affect the activity of MOB (as noted in sections 1.4.4 - 1.4.7). Measuring the potential methane oxidation rate of the biofilter soils can provide information on the activity of the MOB. This can be combined with SIP to potentially illuminate which members of MOB assemblage are active. Plants also seem to effect microbial community composition. Since plants were present on the MBF during the summer months, examining the rhizosphere bacterial communities and the plant species present could yield interesting results.

4.4 Conclusions

In summary, evidence from this study indicates that presence or absence of methane influences the MOB assemblage within a biofilter as well as the total bacterial community composition. DGGE and T-RFLP analysis of the bacterial community demonstrated that shifts in bacterial community occurred when methane was present or absent. qPCR analysis of the 16S rRNA gene indicates that the methane biofilter community was at least partly dependent on methane as a carbon and energy input and that the community declined when methane input ceased. The MOB species diversity remained stable despite the changes in methane input, but based on the qPCR data, the number of MOB did decline in the absence of methane. This decline in the number of MOB could explainthe decline observed in the 16S rRNA gene qPCR data. The MOB species richness did change between sampling dates, with the most diverse assemblage detected at the beginning of phase 2, no methane input. The major members of the MOB assemblage were species related to *Methylomicrobium* and

Methylobacter. The two less abundant assemblage members were related to the *Methylocystis* and *Methylocaldum* genera. The methane biofilter itself functioned properly as no methane emissions were detected and the function of the methane biofilter was preserved even after not receiving a methane input for 2 months.

To the best of our knowledge, this study presents the first temporal analysis of a pilot scale methane biofilter bacterial and MOB community. This includes the first sequenced *pmoA* genes from MOB residing within a methane biofilter. The study also presents novel information about how MOB and bacterial communities respond to changes in methane input in methane biofilter systems. In general this study adds to the body of literature supporting the effectiveness of methane biofilter in mitigating methane emissions from anthropogenic sources.

5.0 REFERENCES

1. **Stocker, Thomas F., Dahe Qin, Gian-Kasper Plattner, Melinda M.B. Tignor, Simon K. Allen, Judith Boschung, Alexander Nauels, Yu Xia, Vincent Bex and PMM**. 2013. CLIMATE CHANGE 2013: The Physical Science Basis. Intergovernmental Panel on Climate Change.

2. **Dalton H**. 2005. The Leeuwenhoek Lecture 2000 the natural and unnatural history of methane-oxidizing bacteria. Philos. Trans. R. Soc. Lond. B. Biol. Sci. **360**:1207–22.

3. **Wolff E, Spahni R**. 2007. Methane and nitrous oxide in the ice core record. Philos. Trans. A. Math. Phys. Eng. Sci. **365**:1775–92.

4. **Ruddiman WF, Thomson JS**. 2001. The case for human causes of increased atmospheric CH 4 over the last 5000 years. Quat. Sci. Rev. **20**:1769–1777.

5. **Ruddiman WF**. 2007. THE EARLY ANTHROPOGENIC HYPOTHESIS : CHALLENGES AND RESPONSES. Holocene 1–37.

6. **Salinger MJ**. 2007. Agriculture's influence on climate during the Holocene. Agric. For. Meteorol. **142**:96–102.

7. **Kutzbach JE, Ruddiman WF, Vavrus SJ, Philippon G**. 2009. Climate model simulation of anthropogenic influence on greenhouse-induced climate change (early agriculture to modern): the role of ocean feedbacks. Clim. Change **99**:351–381.

8. **Conrad R**. 2009. Minireview The global methane cycle : recent advances in understanding the microbial processes involved. Environ. Microbiol. **1**:285–292.

9. **Thauer RK, Kaster A-K, Seedorf H, Buckel W, Hedderich R**. 2008. Methanogenic archaea: ecologically relevant differences in energy conservation. Nat. Rev. Microbiol. **6**:579–91.

10. **Ferry JG**. 1992. Biochemistry of Methanogenesis. Crit. Rev. Biochem. Mol. Biol. **27**:473–503.

11. **Costa KC, Leigh J a**. 2014. Metabolic versatility in methanogens. Curr. Opin. Biotechnol. **29C**:70–75.

12. **Reagan MT, Moridis GJ, Elliott SM, Maltrud M**. 2011. Contribution of oceanic gas hydrate dissociation to the formation of Arctic Ocean methane plumes. Arctic **116**:1–11.

13. **Kroeger KF, di Primio R, Horsfield B**. 2011. Atmospheric methane from organic carbon mobilization in sedimentary basins — The sleeping giant? Earth-Science Rev. **107**:423–442.

14. **Archer D, Buffett B, Brovkin V**. 2009. Ocean methane hydrates as a slow tipping point in the global carbon cycle. Proc. Natl. Acad. Sci. U. S. A. **106**:20596–601.

15. **Kennedy M, Mrofka D, von der Borch C**. 2008. Snowball Earth termination by destabilization of equatorial permafrost methane clathrate. Nature **453**:642–5.

16. **Kemp DB, Coe AL, Cohen AS, Schwark L**. 2005. Astronomical pacing of methane release in the Early Jurassic period. Nature **437**:396–9.

17. **Pancost RD, Steart DS, Handley L, Collinson ME, Hooker JJ, Scott AC, Grassineau N V, Glasspool IJ**. 2007. Increased terrestrial methane cycling at the Palaeocene-Eocene thermal maximum. Nature **449**:332–5.

18. **Elliott S, Maltrud M, Reagan M, Moridis G, Cameron-Smith P**. 2011. Marine methane cycle simulations for the period of early global warming. J. Geophys. Res. **116**:1–13.

19. **Foster JW, Davis RH**. 1966. A methane-dependent coccus, with notes on classification and nomenclature of obligate, methane-utilizing bacteria. J. Bacteriol. **91**:1924–31.

20. **Hanson RS, Hanson TE**. 1996. Methanotrophic bacteria. Microbiol. Rev. **60**:439–71.

21. **Kim TG, Lee E-H, Cho K-S**. 2013. Effects of nonmethane volatile organic compounds on microbial community of methanotrophic biofilter. Appl. Microbiol. Biotechnol. **97**:6549–59.

22. **Ménard C, Ramirez AA, Nikiema J, Heitz M**. 2012. Biofiltration of methane and trace gases from landfills : A review **53**:40–53.

23. **Islam T, Jensen S, Reigstad LJ, Larsen Ø, Birkeland N**. 2008. Methane oxidation at 55 ^{o} C and pH 2 by a thermoacidophilic bacterium belonging to the Verrucomicrobia phylum. Islam Zeitschrift Für Geschichte Und Kult. Des Islam. Orients.

24. **Dunfield PF, Yuryev A, Senin P, Smirnova A V, Stott MB, Hou S, Ly B, Saw JH, Zhou Z, Ren Y, Wang J, Mountain BW, Crowe MA, Weatherby TM, Bodelier PLE, Liesack W, Feng L, Wang L, Alam M**. 2007. Methane oxidation by an extremely acidophilic bacterium of the phylum *Verrucomicrobia.* Nature **450**:879–883.

25. **Pol A, Heijmans K, Harhangi HR, Tedesco D, Jetten MSM, Camp HJMO Den**. 2007. Methanotrophy below pH 1 by a new Verrucomicrobia species. Nature **450**:874–879.

26. **Ettwig KF, van Alen T, van de Pas-Schoonen KT, Jetten MSM, Strous M**. 2009. Enrichment and molecular detection of denitrifying methanotrophic bacteria of the NC10 phylum. Appl. Environ. Microbiol. **75**:3656–62.

27. **Gebert J, Singh BK, Pan Y, Bodrossy L**. 2009. Activity and structure of methanotrophic communities in landfill cover soils. Environ. Microbiol. Rep. **1**:414–423.

28. **Gebert J, Stralis-Pavese N, Alawi M, Bodrossy L**. 2008. Analysis of methanotrophic communities in landfill biofilters using diagnostic microarray. Environ. Microbiol. **10**:1175–88.

29. **Gebert J, Gröngröft A, Schloter M, Gattinger A**. 2004. Community structure in a methanotroph biofilter as revealed by phospholipid fatty acid analysis. FEMS Microbiol. Lett. **240**:61–8.

30. **Jugnia L-B, Aït-Benichou S, Fortin N, Cabral AR, Greer CW**. 2009. Diversity and Dynamics of Methanotrophs within an Experimental Landfill Cover Soil. Soil Sci. Soc. Am. J. **73**:1479.

31. **Wise MG, McArthur J V, Shimkets LJ**. 1999. Methanotroph diversity in landfill soil: isolation of novel type I and type II methanotrophs whose presence was suggested by culture-independent 16S ribosomal DNA analysis. Appl. Environ. Microbiol. **65**:4887–97.

32. **Wise MG, Mcarthur JV, Shimkets LJ**. 2001. Methylosarcina quisquiliarum sp . nov ., novel type I methanotrophs. Int. J. Syst. Evol. Microbiol. 611–621.

33. **Kojima H, Tsutsumi M, Ishikawa K, Iwata T, Mußmann M, Fukui M**. 2012. Distribution of putative denitrifying methane oxidizing bacteria in sediment of a freshwater lake, Lake Biwa. Syst. Appl. Microbiol. **35**:233–8.

34. **Sharp CE, Stott MB, Dunfield PF**. 2012. Detection of autotrophic verrucomicrobial methanotrophs in a geothermal environment using stable isotope probing. Front. Microbiol. **3**:303.

35. **Lieberman RL, Rosenzweig AC**. 2005. Crystal structure of a membrane-bound metalloenzyme that catalyses the biological oxidation of methane. Nature **434**:177–82.

36. **Lieberman RL, Rosenzweig AC**. 2004. Biological methane oxidation: regulation, biochemistry, and active site structure of particulate methane monooxygenase. Crit. Rev. Biochem. Mol. Biol. **39**:147–64.

37. **Hakemian AS, Kondapalli KC, Telser J, Hoffman BM, Stemmler TL, Rosenzweig AC**. 2008. The Metal Centers of Particulate Methane Monooxygenase from Methylosinus 6793–6801.

38. **Smith SM, Rawat S, Telser J, Hoffman BM, Stemmler TL, Rosenzweig AC**. 2011. Crystal structure and characterization of particulate methane monooxygenase from *Methylocystis* species strain M. Biochemistry **50**:10231–40.

39. **Rahman MT, Crombie A, Chen Y, Stralis-Pavese N, Bodrossy L, Meir P, McNamara NP, Murrell JC**. 2011. Environmental distribution and abundance of the facultative methanotroph Methylocella. ISME J. **5**:1061–6.

40. **Semrau JD, Jagadevan S, Dispirito A a, Khalifa A, Scanlan J, Bergman BH, Freemeier BC, Baral BS, Bandow NL, Vorobev A, Haft DH, Vuilleumier S, Murrell JC**. 2013. Methanobactin and MmoD work in concert to act as the "copper-switch" in methanotrophs. Environ. Microbiol. **15**:3077–3086.

41. **Semrau JD, DiSpirito A a, Yoon S**. 2010. Methanotrophs and copper. FEMS Microbiol. Rev. **34**:496–531.

42. **Erikstad H-A, Jensen S, Keen TJ, Birkeland N-K**. 2012. Differential expression of particulate methane monooxygenase genes in the verrucomicrobial methanotroph "*Methylacidiphilum kamchatkense*" Kam1. Extremophiles.

43. **Hakemian AS, Rosenzweig AC**. 2007. The biochemistry of methane oxidation. Annu. Rev. Biochem. **76**:223–41.

44. **Colby BJ, Stirling DI, Dalton H**. 1977. The Soluble Methane Mono-oxygenase of *Methylococcus capsulatus* (Bath). Biochemistry **165**:395–402.

45. **Lee S-W, Im J, Dispirito A a, Bodrossy L, Barcelona MJ, Semrau JD**. 2009. Effect of nutrient and selective inhibitor amendments on methane oxidation, nitrous oxide production, and key gene presence and expression in landfill cover soils: characterization of the role of methanotrophs, nitrifiers, and denitrifiers. Appl. Microbiol. Biotechnol. **85**:389–403.

46. **Tavormina PL, Orphan VJ, Kalyuzhnaya MG, Jetten MSM, Klotz MG**. 2011. A novel family of functional operons encoding methane/ammonia monooxygenase-related proteins in gammaproteobacterial methanotrophs. Environ. Microbiol. Rep. **3**:91–100.

47. **Kip N, Ouyang W, van Winden J, Raghoebarsing A, van Niftrik L, Pol A, Pan Y, Bodrossy L, van Donselaar EG, Reichart G-J, Jetten MSM, Damsté JSS, Op den Camp HJM**. 2011. Detection, isolation, and characterization of acidophilic methanotrophs from Sphagnum mosses. Appl. Environ. Microbiol. **77**:5643–54.

48. **Saidi-Mehrabad A, He Z, Tamas I, Sharp CE, Brady AL, Rochman FF, Bodrossy L, Abell GC, Penner T, Dong X, Sensen CW, Dunfield PF**. 2013. Methanotrophic bacteria in oilsands tailings ponds of northern Alberta. ISME J. **7**:908–21.

49. **Schmidt S, Christen P, Kiefer P, Vorholt J a**. 2010. Functional investigation of methanol dehydrogenase-like protein XoxF in *Methylobacterium extorquens* AM1. Microbiology **156**:2575–86.

50. **Chistoserdova L and MEL**. 1997. Molecular and mutational analysis of a DNA region seperating two methylotrophy gene in *Methylobacterium extorquens* AM1. Microbiology **143**:1729–1736.

51. **Wilson SM, Gleisten MP, Donohue TJ**. 2008. Identification of proteins involved in formaldehyde metabolism by *Rhodobacter sphaeroides*. Microbiology **154**:296–305.

52. **Mustakhimov I, Kalyuzhnaya MG, Lidstrom ME, Chistoserdova L**. 2013. Insights into denitrification in *Methylotenera mobilis* from denitrification pathway and methanol metabolism mutants. J. Bacteriol. **195**:2207–11.

53. **Kalyuzhnaya MG, Hristova KR, Lidstrom ME, Chistoserdova L**. 2008. Characterization of a novel methanol dehydrogenase in representatives of Burkholderiales: implications for environmental detection of methylotrophy and evidence for convergent evolution. J. Bacteriol. **190**:3817–23.

54. **Pol A, Barends TRM, Dietl A, Khadem AF, Eygensteyn J, Jetten MSM, Op den Camp HJM**. 2014. Rare earth metals are essential for methanotrophic life in volcanic mudpots. Environ. Microbiol. **16**:255–64.

55. **Hibi Y, Asai K, Arafuka H, Hamajima M, Iwama T, Kawai K**. 2011. Molecular structure of La3+-induced methanol dehydrogenase-like protein in *Methylobacterium radiotolerans*. J. Biosci. Bioeng. **111**:547–9.

56. **Zahn JA, Bergmann DJ, Boyd JM, Kunz C, Dispirito AA, Spirito AADI**. 2001. Membrane-Associated Quinoprotein Formaldehyde Dehydrogenase from *Methylococcus capsulatus* Bath Membrane-Associated Quinoprotein Formaldehyde Dehydrogenase from Methylococcus capsulatus Bath.

57. **Trotsenko Y a, Murrell JC**. 2008. Metabolic aspects of aerobic obligate methanotrophy. Adv. Appl. Microbiol. **63**:183–229.

58. **Malashenko IP, Pirog TP, Romanovskaia V a, Sokolov IG, Gringerg T a**. 2001. [Search for methanotrophic producers of exopolysaccharides]. Prikl. Biokhim. Mikrobiol. **37**:702–5.

59. **Asenjo JA, Suk JS**. 1986. Microbial Conversion of Methane into Poly- / ~ -Hydroxybutyrate (PHB): Growth and Intracellular Product Accumulation in a Type II Methanotroph. J. Ferment. Technol. **64**:271–278.

60. **Pieja AJ, Rostkowski KH, Criddle CS**. 2011. Distribution and selection of poly-3-hydroxybutyrate production capacity in methanotrophic proteobacteria. Microb. Ecol. **62**:564–73.

61. **Baxter NJ, Hirt RP, Bodrossy L, Kovacs KL, Embley TM, Prosser JI, Murrell JC**. 2002. The ribulose-1,5-bisphosphate carboxylase/oxygenase gene cluster of *Methylococcus capsulatus* (Bath). Arch. Microbiol. **177**:279–89.

62. **Khadem AF, Pol A, Wieczorek A, Mohammadi SS, Francoijs K-J, Stunnenberg HG, Jetten MSM, Op den Camp HJM**. 2011. Autotrophic methanotrophy in verrucomicrobia: *Methylacidiphilum fumariolicum* SolV uses the Calvin-Benson-Bassham cycle for carbon dioxide fixation. J. Bacteriol. **193**:4438–46.

63. **Rasigraf O, Kool DM, Jetten MSM, Sinninghe Damsté JS, Ettwig KF**. 2014. Autotrophic carbon dioxide fixation via the Calvin-Benson-Bassham cycle by the denitrifying methanotroph *Methylomirabilis oxyfera*. Appl. Environ. Microbiol.

64. **Khadem AF, van Teeseling MCF, van Niftrik L, Jetten MSM, Op den Camp HJM, Pol A**. 2012. Genomic and Physiological Analysis of Carbon Storage in the Verrucomicrobial Methanotroph “Ca. *Methylacidiphilum fumariolicum*” SolV. Front. Microbiol. **3**:345.

65. **Semrau JD, DiSpirito A a, Vuilleumier S**. 2011. Facultative methanotrophy: false leads, true results, and suggestions for future research. FEMS Microbiol. Lett. **323**:1–12.

66. **Kalyuzhnaya MG, Yang S, Rozova ON, Smalley NE, Clubb J, Lamb a, Gowda G a N, Raftery D, Fu Y, Bringel F, Vuilleumier S, Beck D a C, Trotsenko Y a, Khmelenina VN, Lidstrom ME**. 2013. Highly efficient methane biocatalysis revealed in a methanotrophic bacterium. Nat. Commun. **4**:2785.

67. **Auman AJ, Speake CC, Lidstrom ME, Auman ANNJ**. 2001. nifH Sequences and Nitrogen Fixation in Type I and Type II Methanotrophs. Appl. Environ. Microbiol. **67**:4009–4016.

68. **Khadem AF, Pol A, Jetten MSM, Op den Camp HJM**. 2010. Nitrogen fixation by the verrucomicrobial methanotroph "*Methylacidiphilum fumariolicum*" SolV. Microbiology **156**:1052–9.

69. **Holmes a J, Costello a, Lidstrom ME, Murrell JC**. 1995. Evidence that particulate methane monooxygenase and ammonia monooxygenase may be evolutionarily related. FEMS Microbiol. Lett. **132**:203–8.

70. **Stein LY, Klotz MG**. 2011. Nitrifying and denitrifying pathways of methanotrophic bacteria. Biochem. Soc. Trans. **39**:1826–31.

71. **Scheutz C, Kjeldsen P, Bogner JE, Visscher A De, Gebert J, Hilger HA, Spokas K, De Visscher A, Huber-Humer M**. 2009. Microbial methane oxidation processes and technologies for mitigation of landfill gas emissions. Waste Manag. Res. **27**:409–55.

72. **King GM, Schnell S**. 1994. Effect of increasing atmospheric methane concentration on ammonium inhibition of soil methane consumption. Nature **370**:282–284.

73. **Scheutz C, Kjeldsen P**. 2004. Environmental factors influencing attenuation of methane and hydrochlorofluorocarbons in landfill cover soils. J. Environ. Qual. **33**:72–9.

74. **Streese J, Stegmann R**. 2003. Microbial oxidation of methane from old landfills in biofilters. Waste Manag. **23**:573–80.

75. **Gebert J, Gröngröft a**. 2006. Performance of a passively vented field-scale biofilter for the microbial oxidation of landfill methane. Waste Manag. **26**:399–407.

76. **Pawłowska M, Rożej A, Stępniewski W**. 2011. The effect of bed properties on methane removal in an aerated biofilter--model studies. Waste Manag. **31**:903–13.

77. **Wilshusen JH, Hettiaratchi JP a, De Visscher a, Saint-Fort R**. 2004. Methane oxidation and formation of EPS in compost: effect of oxygen concentration. Environ. Pollut. **129**:305–14.

78. **Wilshusen JH, Hettiaratchi JP a, Stein VB**. 2004. Long-term behavior of passively aerated compost methanotrophic biofilter columns. Waste Manag. **24**:643–53.

79. **Scheutz C, Kjeldsen P, Bogner JE, Visscher A De, Gebert J, Hilger HA, Spokas K**. 2009. Waste Management & Research technologies for mitigation of landfill gas emissions. Waste Manag. Res. **27**.

80. **Börjesson G, Sundh I, Svensson B**. 2004. Microbial oxidation of CH(4) at different temperatures in landfill cover soils. FEMS Microbiol. Ecol. **48**:305–12.

81. **Hettiarachchi VC, Hettiaratchi PJ, Mehrotra AK, Kumar S**. 2011. Field-scale operation of methane biofiltration systems to mitigate point source methane emissions. Environ. Pollut. **159**:1715–20.

82. **Bodelier PLE, Laanbroek HJ**. 2004. Nitrogen as a regulatory factor of methane oxidation in soils and sediments. FEMS Microbiol. Ecol. **47**:265–77.

83. **Boeckx P, Cleemput O Van, Villaralvo I**. 1996. Methane emission from a landfill and the methane oxidising capacity of its covering soil. Soil Biol. Biochem. **28**:1397–1405.

84. **Hilger H, Wollum AG, Barlaz MA**. 2000. Landfill methane oxidation response to vegetation, fertilization, and liming. J. Environ. Qual. **29**:324–334.

85. **Veillette M, Viens P, Ramirez AA, Brzezinski R, Heitz M**. 2011. Effect of ammonium concentration on microbial population and performance of a biofilter treating air polluted with methane. Chem. Eng. J. **171**:1114–1123.

86. **Bodelier PL, Roslev P, Henckel T, Frenzel P**. 2000. Stimulation by ammonium-based fertilizers of methane oxidation in soil around rice roots. Nature **403**:421–4.

87. **Bodelier PLE, Hahn AP, Arth IR**. 2000. Effects of ammonium-based fertilisation on microbial processes involved in methane emission from soils planted with rice. Biogeochemistry **51**:225–257.

88. **Im J, Lee S-W, Bodrossy L, Barcelona MJ, Semrau JD**. 2011. Field application of nitrogen and phenylacetylene to mitigate greenhouse gas emissions from landfill cover soils: effects on microbial community structure. Appl. Microbiol. Biotechnol. **89**:189–200.

89. **Borjesson G**. 2001. Inhibition of methane oxidation by volatile sulfur compounds (CH_3SH and CS_2) in landfill cover soils. Waste Manag. Res. **19**:314–319.

90. **Nikiema J, Brzezinski R, Heitz M**. 2010. Influence of phosphorus, potassium, and copper on methane biofiltration performanceA paper submitted to the Journal of Environmental Engineering and Science. Can. J. Civ. Eng. **37**:335–345.

91. **Mohanty SR, Bharati K, Deepa N, Rao VR, Adhya TK**. 2000. Influence of heavy metals on methane oxidation in tropical rice soils. Ecotoxicol. Environ. Saf. **47**:277–84.

92. **Van der Ha D, Hoefman S, Boeckx P, Verstraete W, Boon N**. 2010. Copper enhances the activity and salt resistance of mixed methane-oxidizing communities. Appl. Microbiol. Biotechnol. **87**:2355–63.

93. **Griffiths RI, Whiteley AS, Anthony G, Donnell O, Bailey MJ, Donnell AGO**. 2000. Rapid Method for Coextraction of DNA and RNA from Natural Environments for Analysis of Ribosomal DNA- and rRNA-Based Microbial Community Composition Rapid Method for Coextraction of DNA and RNA from Natural Environments for Analysis of Ribosomal DNA- and 1–5.

94. **Miller DN, Bryant JE, Madsen EL, Ghiorse WC**. 1999. Evaluation and optimization of DNA extraction and purification procedures for soil and sediment samples. Appl. Environ. Microbiol. **65**:4715–24.

95. **Steven B, Briggs G, McKay CP, Pollard WH, Greer CW, Whyte LG**. 2007. Characterization of the microbial diversity in a permafrost sample from the Canadian high Arctic using culture-dependent and culture-independent methods. FEMS Microbiol. Ecol. **59**:513–23.

96. **Auman AJ, Stolyar S, Costello AM, Lidstrom E, Auman ANNJ**. 2000. Molecular Characterization of Methanotrophic Isolates from Freshwater Lake Sediment Molecular Characterization of Methanotrophic Isolates from Freshwater Lake Sediment. Appl. Environ. Microbiol. **66**:5259–5266.

97. **Wang Y, Wu W, Ding Y, Liu W, Perera A, Chen Y, Devare M**. 2008. Methane oxidation activity and bacterial community composition in a simulated landfill cover soil is influenced by the growth of *Chenopodium album* L. Soil Biol. Biochem. **40**:2452–2459.

98. **Shelley F, Grey J, Trimmer M, B PRS**. 2014. Widespread methanotrophic primary production in lowland chalk rivers. Proceedings of the Royal Society. **281:** 20132854

iks a. J, Leuven RSEW, Middelburg JJ, van der Velde G, Verberk WCEP. 2013. Methane as a carbon source for the food web in raised bog pools. Freshw. Sci. **32**:1260–1272.

100. **Kim TG, Jeong S-Y, Cho K-S**. 2013. Functional rigidity of a methane biofilter during the temporal microbial succession. Appl. Microbiol. Biotechnol. 3275–3286.

101. **Cébron A, Bodrossy L, Chen Y, Singer AC, Thompson IP, Prosser JI, Murrell JC**. 2007. Identity of active methanotrophs in landfill cover soil as revealed by DNA-stable isotope probing. FEMS Microbiol. Ecol. **62**:12–23.

102. **Chi Z, Lu W, Mou Z, Wang H, Long Y, Duan Z**. 2012. Effect of biocover equipped with a novel passive air diffusion system on microbial methane oxidation and community of methanotrophs. J. Air Waste Manage. Assoc. **62**:278–286.

103. **Ait-Benichou S, Jugnia L-B, Greer CW, Cabral AR**. 2009. Methanotrophs and methanotrophic activity in engineered landfill biocovers. Waste Manag. **29**:2509–17.

104. **Héry M, Singer AC, Kumaresan D, Bodrossy L, Stralis-Pavese N, Prosser JI, Thompson IP, Murrell JC**. 2008. Effect of earthworms on the community structure of active methanotrophic bacteria in a landfill cover soil. ISME J. **2**:92–104.

105. **Li H, Chi Z, Lu W, Wang H**. 2014. Sensitivity of methanotrophic community structure, abundance, and gene expression to CH4 and O2 in simulated landfill biocover soil. Environ. Pollut. **184**:347–53.

106. **Pan Y, Abell GCJ, Bodelier PLE, Meima-Franke M, Sessitsch A, Bodrossy L**. 2014. Remarkable Recovery and Colonization Behaviour of Methane Oxidizing Bacteria in Soil After Disturbance Is Controlled by Methane Source Only. Microb. Ecol.

107. **Pieja AJ, Sundstrom ER, Criddle CS**. 2011. Poly-3-hydroxybutyrate metabolism in the type II methanotroph *Methylocystis parvus* OBBP. Appl. Environ. Microbiol. **77**:6012–9.

108. **Roslev P, King GM**. 1994. Survival and Recovery of Methanotrophic Bacteria Starved under Oxic and Anoxic Conditions Survival and Recovery of Methanotrophic Bacteria Starved under Oxic and Anoxic Conditionst **60**.

109. **Roslev P, King GM, Roslev P, King GM**. 1995. Aerobic and anaerobic starvation metabolism in methanotrophic bacteria . These include : Aerobic and Anaerobic Starvation Metabolism in Methanotrophic Bacteria † **61**.

110. **Schnell S, King GM**. 1995. Stability of methane oxidation capacity to variations in methane and nutrient concentrations. FEMS Microbiol. Ecol. **17**:285–294.

111. **Cox HHJ, Deshusses M a**. 2002. Effect of starvation on the performance and re-acclimation of biotrickling filters for air pollution control. Environ. Sci. Technol. **36**:3069–73.

112. **Wani AH, Branion RMR, Lau AK**. 1998. Effects of periods of starvation and fluctuating hydrogen sulfide concentration on biofilter dynamics and performance. J. Hazard. Mater. **60**:287–303.

113. **Bowman JP**. 2011. Approaches for the characterization and description of novel methanotrophic bacteria.Methods in enzymology, 1st ed. Elsevier Inc.

114. **Nielsen PH, Nielsen JL, Baranyi C, Stoecker K, Bendinger B, Toenshoff ER, Daims H, Wagner M**. 2006. Cohn ' s Crenothrix is a filamentous methane oxidizer with an unusual methane monooxygenase. PNAS **103**:2363–2367.

115. **Ettwig KF, Butler MK, Paslier D Le, Pelletier E, Mangenot S, Kuypers MMM, Schreiber F, Dutilh BE, Zedelius J, Beer D De, Gloerich J, Wessels HJCT, Alen T Van, Luesken F, Wu ML, Pas-schoonen KT Van De, Camp HJMO Den, Janssen-Megens EM, Francoijs K-J, Stunnenberg H, Weissenbach J, Jetten MSM, Strous M, Le Paslier D, de Beer D, van Alen T, van de Pas-Schoonen KT, Op den Camp HJM**. 2010. Nitrite-driven anaerobic methane oxidation by oxygenic bacteria. Nature **464**:543–8.

116. **Case RJ, Boucher Y, Dahllöf I, Holmström C, Doolittle WF, Kjelleberg S**. 2007. Use of 16S rRNA and rpoB genes as molecular markers for microbial ecology studies. Appl. Environ. Microbiol. **73**:278–88.

117. **Reim A, Lüke C, Krause S, Pratscher J, Frenzel P**. 2012. One millimetre makes the difference: high-resolution analysis of methane-oxidizing bacteria and their specific activity at the oxic-anoxic interface in a flooded paddy soil. ISME J. **6**:2128–39.

118. **Semrau JD, Chistoserdov A, Lebron J, Costello A, Davagnino J, Kenna E, Holmes AJ, Finch R, Murrell JC, Lidstrom ME, Semrau JD, Chistoserdov A, Lebron J, Costello A, Davagnino J, Kenna E**. 1995. Particulate methane monooxygenase genes in methanotrophs . Particulate Methane Monooxygenase Genes in Methanotrophs **177**.